Stray particles as the source of residuals in sand filtrate: Behavior of superfine powdered activated carbon particles in water treatment processes

Yoshifumi Nakazawa [a], Taketo Abe [a], Yoshihiko Matsui [b]*, Nobutaka Shirasaki [b], and Taku Matsushita [b]

a Graduate School of Engineering, Hokkaido University, N13W8, Sapporo 060-8628, Japan
b Faculty of Engineering, Hokkaido University, N13W8, Sapporo 060-8628, Japan

* Corresponding author. Tel./fax: +81-11-706-7280
E-mail address: matsui@eng.hokudai.ac.jp

Abstract

Although superfine powdered activated carbon has excellent adsorption properties, it is not used in conventional water treatment processes comprising coagulation–flocculation, sedimentation, and sand filtration (CSF) due to concerns about its residual in treated water. Here, we examined the production and fate of very fine carbon particles with lacking in charge neutralization as a source of the residual in sand filtrate after CSF treatment. Almost all of the carbon particles in the water were charge-neutralized by coagulation treatment with rapid mixing, but a very small amount (≤0.4% of the initial concentration) of very fine carbon particles with a lesser degree of charge neutralization were left behind in coagulation process. Such carbon particles, defined as stray carbon particles, were hardly removed by subsequent flocculation and sedimentation processes, and some of them remained in the sand filtrate. The concentration of residual carbon particles in the sand filtrate varied similarly with that of the stray carbon particles. The stray and residual carbon particles were similarly smaller than the particles before coagulation treatment, but the residual carbon particles had less charge neutralization than the stray carbon particles. The turbidity of water samples collected after sedimentation was not correlated with the residual carbon concentration in the sand filtrate, even though it is often used as an indicator of treatment performance with respect to the removal of suspended matter. Based on these findings, we suggest that reduction of the amount of stray particles should be a performance goal of the CSF treatment. Examining this concept further, we confirmed that the residence time distributions in the coagulation and flocculation reactors influenced the concentration of stray carbon particles and then the residual carbon particle concentration in sand filtrate, but found that the effect was dependent on coagulant type. A multi-chambered-reactor configuration lowered both the stray carbon particle concentration after coagulation treatment and the residual carbon particle concentration in sand filtrate compared with a single-chambered reactor configuration. When a normal basicity PACl that consisted mainly of monomeric Al species was used, the stray carbon particle concentration was decreased during coagulation process and then gradually decreased during subsequent flocculation process because the monomeric Al species were transformed to colloidal Al species via polymeric Al species. In contrast, when a high-basicity PACl that consisted mostly of colloidal Al species was used, coagulation treatment largely decreased the stray carbon particle concentration, which did not decrease further during subsequent flocculation process. These findings will be valuable for controlling residual carbon particles after the CSF treatment.

Keywords

SPAC; PACl; aluminum species; filtration; turbidity

Research highlights

A very small portion (≤0.4%) of influent SPAC were left behind in coagulation

These stray particles drastically decreased only during early stage of coagulation

They barely decrease during flocculation to sedimentation and reside in sand filtrate

Stray particles had smaller size and less charge neutralization

Measures to effectively reduces stray particles were discussed

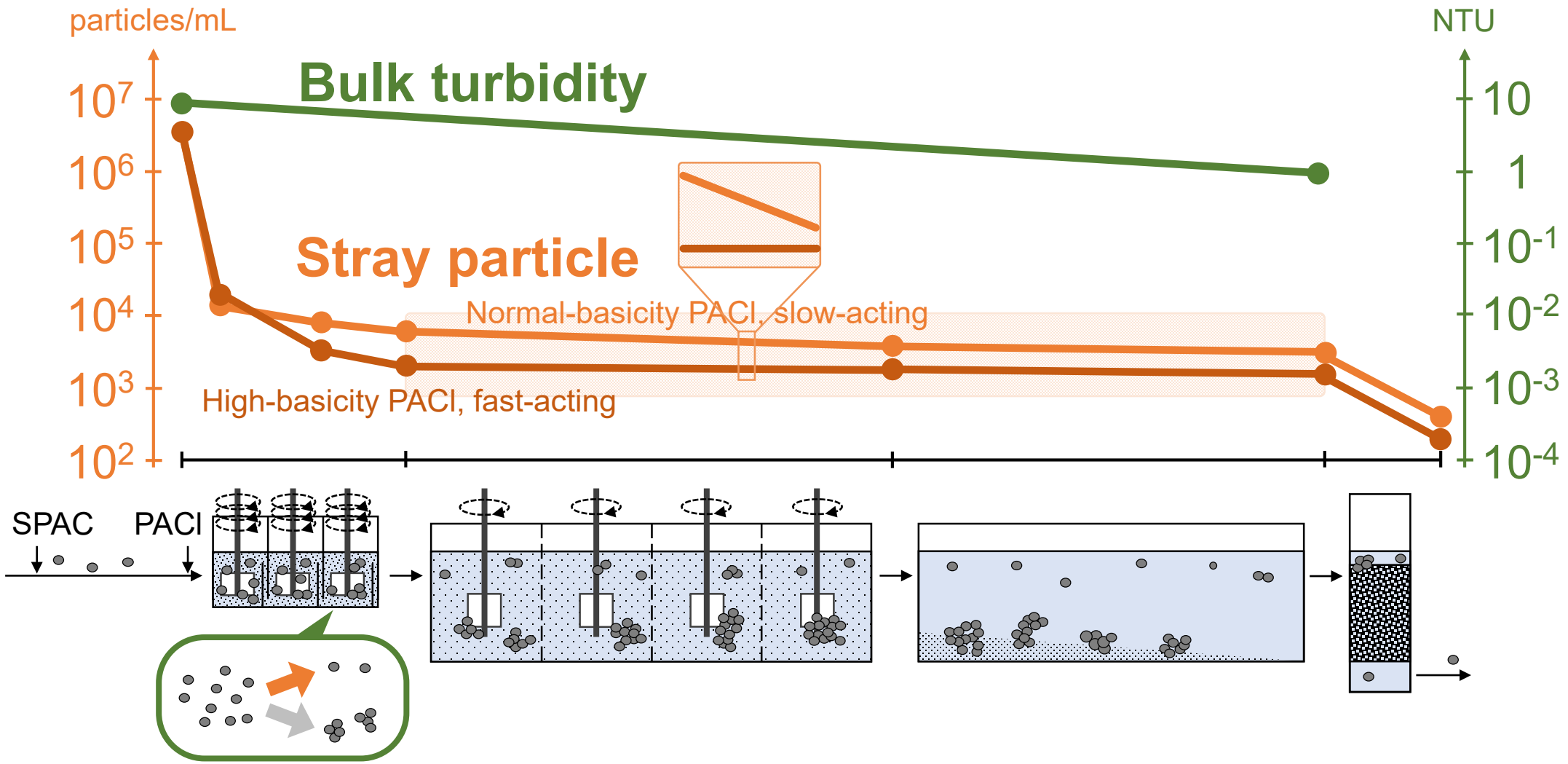
particles/mL
NTU
Bulk turbidity
Stray particle
Normal-basicity PACI, slow-acting
High-basicity PACI, fast-acting
10^7
10^6
10^5
10^4
10^3
10^2
10
1
10^{-1}
10^{-2}
10^{-3}
10^{-4}
SPAC
PACI

Stray particles as the source of residuals in sand filtrate: Behavior of superfine powdered activated carbon particles in water treatment processes

Yoshifumi Nakazawa [a], Taketo Abe [a], Yoshihiko Matsui [b]*, Nobutaka Shirasaki [b], and Taku Matsushita [b]

a Graduate School of Engineering, Hokkaido University, N13W8, Sapporo 060-8628, Japan
b Faculty of Engineering, Hokkaido University, N13W8, Sapporo 060-8628, Japan

* Corresponding author. Tel./fax: +81-11-706-7280
E-mail address: matsui@eng.hokudai.ac.jp

Abstract

Although superfine powdered activated carbon has excellent adsorption properties, it is not used in conventional water treatment processes comprising coagulation–flocculation, sedimentation, and sand filtration (CSF) due to concerns about its residual in treated water. Here, we examined the production and fate of very fine carbon particles with lacking in charge neutralization as a source of the residual in sand filtrate after CSF treatment. Almost all of the carbon particles in the water were charge-neutralized by coagulation treatment with rapid mixing, but a very small amount (≤0.4% of the initial concentration) of very fine carbon particles with a lesser degree of charge neutralization were left behind in coagulation process. Such carbon particles, defined as stray carbon particles, were hardly removed by subsequent flocculation and sedimentation processes, and some of them remained in the sand filtrate. The concentration of residual carbon particles in the sand filtrate varied similarly with that of the stray carbon particles. The stray and residual carbon particles were similarly smaller than the particles before coagulation treatment, but the residual carbon particles had less charge neutralization than the stray carbon particles. The turbidity of water samples collected after sedimentation was not correlated with the residual carbon concentration in the sand filtrate, even though it is often used as an indicator of treatment performance with respect to the removal of suspended matter. Based on these findings, we suggest that reduction of the amount of stray particles should be a performance goal of the CSF treatment. Examining this concept further, we confirmed that the residence time distributions in the coagulation and flocculation reactors influenced the concentration of stray carbon particles and then the residual carbon particle concentration in sand filtrate, but found that the effect was dependent on coagulant type. A multi-chambered-reactor configuration lowered both the stray carbon particle concentration after coagulation treatment and the residual carbon particle concentration in sand filtrate compared with a single-chambered reactor configuration. When a normal basicity PACl that consisted mainly of monomeric Al species was used, the stray carbon particle concentration was decreased during coagulation process and then gradually decreased during subsequent flocculation process because the monomeric Al species were transformed to colloidal Al species via polymeric Al species. In contrast, when a high-basicity PACl that consisted mostly of colloidal Al species was used, coagulation treatment largely decreased the stray carbon particle concentration, which did not decrease further during subsequent flocculation process. These findings will be valuable for controlling residual carbon particles after the CSF treatment.

Keywords

SPAC; PACl; aluminum species; filtration; turbidity

1. Introduction

Superfine powdered activated carbon (SPAC; median diameter, approx. 1 μm) shows excellent adsorption performance for organic molecules and is drawing attention from researchers and practitioners as a very effective adsorbent for use in water and wastewater treatment processes (Amaral *et al.* 2016, Apul *et al.* 2017, Ateia *et al.* 2019, Bonvin *et al.* 2016, Decrey *et al.* 2020, Matsui *et al.* 2013, Murray *et al.* 2019, Partlan *et al.* 2020). Some full-scale water purification plants that use membrane filtration processes are already using SPAC as an adsorbent (Kanaya *et al.* 2015); however, it is not yet used at plants that use conventional coagulation–flocculation, sedimentation, and sand filtration (CSF) processes. This is because there are concerns that the use of SPAC may result in the finished water's containing a larger concentration of residual carbon particles than the concentration that would result from use of conventionally sized powdered activated carbon (PAC; median diameter, approx. 15 μm) had been used (Nakazawa *et al.* 2018a).

Several studies have been conducted on the removal of activated carbon particles during CSF processes. These studies have focused mainly on particle charge neutralization, the size and growth of floc particles, and the reduction of turbidity after sedimentation and filtration with respect to the use of PAC. For example, it has been reported that the addition of PAC followed by alum coagulation increases turbidity after sedimentation and increases the size and growth rate of floc particles compared to use of only alum coagulation (Huang *et al.* 2020). Similarly, it has been reported that the addition of PAC followed by $FeCl_3$ coagulation decreases floc particle size but leaves the turbidity after sedimentation relatively unchanged compared with treatment with $FeCl_3$ alone (Younker and Walsh 2016). Furthermore, the use of SPAC induces the formation of larger floc particles than use of PAC (Matsui *et al.* 2009). Thus, these studies have demonstrated how floc particles are formed by coagulation and flocculation, and how the coagulation and flocculation processes proceed, so that particles in raw water can be easily removed by sedimentation after coagulation and flocculation.

However, few studies have focused on the residual particles remaining in treated water after sedimentation and filtration. If we examine the size distribution of floc particles (Hu *et al.* 2013, Sun *et al.* 2016, Zhang *et al.* 2008), it may be possible to determine the amount of residual particles. However, such residual particles are present in only very small concentrations at the very extreme ends of the size distribution, making them difficult to be determined using particle distribution data (Lee *et al.* 2009, Yu *et al.* 2015). Indeed, it has been reported that under optimized CSF conditions, very few SPAC particles remain in sand filtrate (only 10^{-5} to 10^{-6} of the particles before treatment) (Nakazawa *et al.* 2018b). In this context, some studies on residual particles have been carried out using microscopy. Aguilar *et al.* (2003) report that the elimination efficiency of particulate matter is increased if PAC is dosed before coagulation process compared to without the use of PAC; however, they also reported that some carbon particles in the size range of 5.5–8.5 μm remained in the treated water (Aguilar et al. 2003).

If coagulation and flocculation are performed well, there should be few residual particles in the treated water. That is because proper coagulation and flocculation results in the formation of large floc particles with good settling properties and water with low turbidity after settling and filtration. However, recent studies have shown that although carbon particles in raw water are effectively charge neutralized by coagulation treatment, resulting in good floc formation, some carbon particles still persist in the sand filtrate and that these particles lack charge neutralization (Nakazawa et al. 2018a, Nakazawa et al. 2018b). This suggests that although the size and settleability of floc particles and the persistence of residual particles in sand filtrate are determined by the performance of the coagulation–flocculation process, they reflect the results of different aspects of the process and are not necessarily interrelated.

Here, we assumed that two types of particles are formed after coagulation: those that can grow into floc particles due to adequate charge neutralization during the coagulation process, and those that cannot grow into floc particles due to insufficient charge neutralization. We then examined the behavior of the latter particles, which were referred as stray particles in this paper, during the CSF process with respect to the amount of residual carbon particles in sand filtrate at the end of the treatment process. The effects of coagulation and flocculation reactor configuration, as well as the type and dose of coagulant used, on the removal of SPAC particles were also investigated.

2. Materials and methods

2.1. Coagulants and activated carbon particles

Two kinds of commercially available poly-aluminum chloride (PACl), provided by Taki Chemical Co., Ltd. (Hyogo, Japan), were used as coagulants: PACl-70 (basicity, 2.1; %basicity, 70%; sulfate ion, 2.2 wt%) and PACl-50 (basicity, 1.5; %basicity, 50%; sulfate ion, 2.9 wt%). The Al speciation (Ala, monomeric Al species; Alb, polymeric Al species; and Alc, colloidal species) distributions of the PACls were determined by the Ferron method (Wang *et al.* 2004), which uses the difference in reaction time with Ferron reagent (8-hydroxy-7-iodoquinoline-5-sulfonic acid; Fujifilm Wako Pure Chemical Corporation, Osaka, Japan) to distinguish between the different Al species. The procedure of Kimura *et al.* (2013) was applied, as described in the Supplementary Information (SI).

SPAC was prepared in our laboratory by wet ball milling (Nikkato, Osaka, Japan) for 6 h followed by wet bead milling for 30 min (LMZ015; Ashizawa Finetech, Ltd., Chiba, Japan), as summarized in the SI and described in detail elsewhere (Pan *et al.* 2017). The concentrations and particle sizes of carbon particles in water samples obtained from the CSF experiment were determined by membrane filtration (nominal pore diameter, 0.1 μm; Φ25 mm; polytetrafluoroethylene; Merck KGaA, Darmstadt, Germany) and microscopic image analysis (1000× magnification; VHX-2000; Keyence Corporation, Osaka, Japan), as summarized in the SI and described in detail elsewhere (Nakazawa et al. 2018a).

2.2. Flow-through reactor tests of coagulation–flocculation, sedimentation, and rapid sand filtration

A series of flow-through mode CSF tests were performed using a bench-scale CSF plant comprising five components: preparation unit, rapid mixing unit for coagulation, slow mixing unit for flocculation, sedimentation unit, and sand filter (Fig. 1 and Table S1). The rapid mixing unit constituted a single-chambered reactor or a 3-chambered-reactor with three equally-sized chambers; the two reactors had the same total hydraulic retention time (HRT) of 100 s. The slow mixing unit constituted a single-chambered reactor or a 4-chambered reactor, both with four mixing impellers and the same total HRT of 2400 s. Regardless of reactor configuration, rapid mixing for coagulation was conducted at a fixed mixing intensity (G value: velocity gradient) of 600 s^{-1} for 100 s, and slow mixing for flocculation was conducted at a fixed G value of 12.5 s^{-1} for 2400 s. Residence time distributions of the reactors were measured via a step tracer test using NaCl as the tracer and conductivity detection (Crittenden *et al.* 2012). To prevent the effects of wind and temperature-induced density current, the bench-scale CSF plant was installed in a constant-temperature room with no wind, and the water temperature was kept at the same as the room temperature.

Toyohira River water, collected at the Moiwa Water Purification Plant, Sapporo, Japan (hereafter 'River water 1'), was used as the raw water. We also used dechlorinated Sapporo municipal water (Municipal waters 1–3 and 5–7; Table S2) because only a limited volume of River water was available. Raw water was pumped into the first mixing chamber of the preparation unit, and SPAC was added in the second mixing chamber at a concentration of 2 mg/L (3–5 × 10^6 particles/mL), which is a typical dose when SPAC is used as an adsorbent (Matsui *et al.* 2007). After the addition of NaOH or HCl to adjust the pH to 7.0, a coagulant (PACl) was injected into the coagulation reactor at a dose of 1.5 mg-Al/L, unless otherwise noted; the dose was predetermined to bring the settling turbidity down to less than 2 NTU. After coagulation–flocculation, the water flowed through a sedimentation reactor, which had a HRT of 65 min. After sedimentation, the supernatant flowed to a sand filter. Sand filtration was conducted at a rate of 90 or 150 m d^{-1} using a 4-cm diameter column filled with sand (effective diameter, 0.94 mm; uniformity, 1.24; Nihon Genryo Co., Ltd., Japan) to a depth of 50 cm.

2.3. Batch tests of coagulation–flocculation

Three series of batch tests were conducted to examine the removal of SPAC by coagulation–flocculation, measure the zeta potential of the carbon particles, and examine changes in the aluminum species distribution during coagulation–flocculation.

To examine SPAC coagulation–flocculation, 1 L of dechlorinated municipal drinking water (Municipal water 1; Table S2) or Wanigawa River water (Ibaraki, Japan; hereafter 'River water 2'; Table S2), was transferred to a rectangular beaker, supplemented with SPAC at a concentration of 2 mg/L, and used for the tests. After adding NaOH (0.05 N) to bring the pH to 7.0, one of the PACls (1.5 mg-Al/L) was injected, and the water was subjected to rapid

mixing (G = 600 s^{-1}) for coagulation; samples of the water were collected at predetermined times and used for analysis. In some tests, after the rapid mixing for 100 s, the water was subjected to slow mixing (G = 12.5 s^{-1}) to flocculation.

To measure zeta potentials, raw water (Municipal water 4; Table S2) was treated as described above, but PACl doses of 1.5 and 2.0 mg-Al/L were used. At 100 s from the start of rapid mixing, a 55-mL sample of water was collected and used for the measurement of the zeta potential (Zetasizer Nano ZS; Malvern, United Kingdom) of the carbon particles; 10 mL was used immediately for the measurement of zeta potential, and the remaining 45 mL was used after being subjected to centrifugal separation (see Section 2.4).

To examine the changes in the aluminum species distributions, raw water (Municipal water 1) was treated as described above, but after adding NaOH to bring the pH to 7.0, one of the PACls was injected at a concentration of 270 mg-Al/L. Rapid mixing (G = 381 s^{-1}) was then conducted without SPAC. Immediately after sampling at predetermined times, the water was used for Ferron analyses with a glass cell (optical path length, 10 cm). The municipal water itself had little effect on the absorbance determined by Ferron analysis (blank test, data not shown).

2.4. Collection of stray particles by centrifugation

In the water samples collected during rapid and slow mixing processes in the flow-through reactor tests and batch tests, particles that had not settled after centrifugation were considered to be stray particles. The centrifuge procedure was as follows. Aliquots (45 mL) of a single water sample were dispensed into four 50-mL glass tubes. The tubes were centrifuged by using a centrifuge (CT6E; Koki Holdings Co., Ltd., Tokyo, Japan) equipped with a swing rotor (T5SS; Koki Holdings Co., Ltd.). Centrifugation was carried out at 4800 rpm (3990*g*) for 10 min, halted, and then re-started for 20, 35, or 50 min (total time, 30, 45, and 60 min, respectively). The reason for the double centrifugation is discussed in Section 3.2. Thereafter, the concentrations of carbon particles in the centrifugal supernatant were determined by membrane filtration and microscopic image analysis (SI).

3. Results and Discussion

3.1. Residual carbon particles after treatment with a bench-scale CSF plant

First, we examined the residual carbon particle concentration in sand filtrate with increasing filtration time using a bench-scale CSF plant, a SPAC dose of 2 mg/L, and PACl-70 as the coagulant at 1.5 or 2.25 mg-Al/L (Fig. 2). At each time point examined, the residual carbon particle concentration was lower when the higher concentration of coagulant was used than when the lower concentration was used. Irrespective of coagulant dose, the residual carbon particle concentration started high and then decreased with increasing filtration time until a steady state was reached at less than 200 particles/mL; this particle concentration is similar to that reported for a full-scale CSF water purification plant using PAC (Kobayashi *et al.* 2019).

The high concentration of particles during the initial period of filtration was not due to residual backwash water remaining in the filter because the filter media was washed with pure water (Milli-Q Advantage A10 System; Merck KGaA) during the final washing process. Therefore, we concluded that the filter underwent a 'ripening' process, which is when clean sand media captures particles that cause the filter to become more efficient at capturing additional particles over time (Crittenden et al. 2012).

Although a clear decrease in residual carbon particle concentration was observed as the filter ripened, no clear change in the particle size distribution of the residual particles was observed (range, 0.3–2 μm; Fig. S1). Therefore, the increased removal of carbon particles with increasing filtration time was not related to the particle size of the carbon particles. In conjunction with our previously reported finding that the carbon particles remaining in sand filtrate had a higher negative charge than the carbon particles entering the sand filter (Nakazawa et al. 2018a), we interpreted this increased removal efficacy as follows. The sand filter treats the sedimentation supernatant, which contains particles with varying degrees of charge neutralization. Clean sand media has a high negative charge (Edzwald 2011), so the charge-neutralized particles attach to the surface of the sand particles and remain in the sand filter. In contrast, the less-charge-neutralized particles are unable to attach to the sand particles due to repulsive forces and therefore exit the filter. However, as the filter ripens by the accumulation of charge-neutralized particles, the ability of the less-charge-neutralized particles to attach to the immobilized charge-neutralized particles results in increased removal efficacy over time. To examine the role of particle attachment in more detail, we conducted experiments at two different filtration rates (Fig. S2) under the assumption that the filtration mechanism comprises two steps: transport, where suspended particles are transported to the surface of sand grains, and attachment, where the particles attach to the sand grains (Edzwald 2011). In our experiments, we observed that the higher filtration rate resulted in higher particle concentrations in the filtrate, suggesting that the higher filtration velocity resulted in decreased attachment efficiency [the number of particle sand-grain adhesions divided by the number of particle sand-grain collisions (Crittenden et al. 2012)] of the carbon particles to the filter.

3.2. Stray particles as the source of the residual particles

As discussed in the previous section, less-charge-neutralized carbon particles with a size of 0.3–2 μm remained in the sand filtrate. We assumed that such particles were particles that had not reacted with the coagulant during the coagulation–flocculation process (we named these particles 'stray particles') and then evaded being captured by the filter media. Based on this assumption, we next examined the relationship between residual carbon particle concentration and stray carbon particle concentration to see whether the stray carbon particle concentration could be used as an index of residual carbon particle concentration. In addition, we examined the effect of coagulant dose on the stray carbon particle concentration and the residual carbon particle concentration in sand filtrate. To do these, we determined the stray particle

concentration in the centrifuged supernatant of water samples collected after coagulation treatment.

First, however, we optimized the conditions used for centrifugal separation. In test trials, we found that preliminary centrifugation for 10 min was sufficient to allow large floc particles to settle. We also found that adhesion to the centrifuge tube wall could be minimized by conducting a second centrifugation after the preliminary centrifugation. In centrifugal separation, a brake is usually applied to stop the rotation of the centrifuge. However, we found that small amounts of the particles were re-suspended by this braking operation. Therefore, we minimized the re-suspension of particles by waiting for the rotation to stop naturally. We also examined how total centrifugation time (the total time for both centrifugation stages) affected residual carbon particle concentration in the supernatant (Fig. S3). We found that the residual carbon particle concentration after centrifugal separation markedly decreased when the centrifuge time was extended from 30 to 45 min, but that it did not further decrease when the time was extended to 60 min. We also found that the particle concentration after centrifugation for 45 min did not vary depending on coagulant dose (Fig. S3b), even though we found that the particle concentration in sand filtrate did vary (Fig. S4). Based on our findings, we used a centrifugal separation time of 30 min to determine stray particle concentrations in the subsequent experiments.

The stray carbon particles and the residual carbon particles were similarly smaller than the particles before the CSF treatment (Fig. S5). The concentrations were decreased with increasing PACl dosage (Fig. 3a). In addition, the stray particle concentration was found to be highly correlated with residual carbon particle concentration in the sand filtrate (R^2 = 0.89, square of Pearson's correlation coefficient). Thus, the stray particle concentration of the supernatant, which was determined after centrifugation for 30 min, was considered an index of the residual particle concentration in the sand filtrate. Furthermore, we found that the concentration of stray particles decreased during coagulation with rapid mixing. After coagulation, the concentration of stray particles (maximum, 1.5×10^4 particles/mL, Fig. 3a) was less than 0.4% that of the initial suspension before coagulation ($3–5 \times 10^6$ particles/mL). We also examined the correlation between the residual carbon particle concentration in the sand filtrate and the turbidity of settled water, which is conventionally used as an indicator of treatment performance with respect to the removal of suspended matter, but we found a lower correlation (R^2 = 0.72) than that found for stray particle concentration (Fig. 3). Thus, stray particle concentration obtained by centrifugation was considered a better index of residual particle concentration than was the turbidity of water. It is important to note here that stray particle concentration was measured at an early stage of the CSF process (after coagulation), whereas turbidity was measured later in the process (after coagulation–flocculation and sedimentation). This suggests that the performance of the coagulation treatment, but not of the flocculation and sedimentation treatment, is the major determinant of the concentration of residual particles remaining after sand filtration. This is discussed further in Section 3.3.

Next, we examined the zeta potentials of bulk particles and stray particles in water samples collected after coagulation (Fig. 4). The bulk particles were charged-neutralized and had zero or only a slightly positive/negative charge. In contrast, the stray particles, which were only a portion of these particles, had a negative charge. This finding that the stray particles had less charge neutralization was similar to the previous researches. Ding *et al.* (2016) report that meso-particles (20 nm–0.5 μm) remained with less charge-neutralization in comparison with the larger floc particles when surface water was treated by coagulation. Yu et al. (2015) report that the zeta potential of the remaining flocs became more negative after sedimentation process. A similar phenomenon was also observed for the residual carbon particles in the sand filtrate, which had less charge neutralization compared with the bulk particles sampled after coagulation (Nakazawa et al. 2018a), although the zeta potentials of the stray particles showed that they had a less-negative charge than did the residual carbon particles. This is thought to be because most of the stray particles with less-negative charges are preferentially removed by the sand filter, as will be discussed in section 3.5.

Together, these findings further support the idea that stray carbon particles are the main source of the residual carbon particles in sand filtrate. This suggests that coagulation–flocculation treatments should be optimized not only to decrease settling turbidity via the formation of large-size floc particles but also to reduce the number of stray particles.

3.3. Effect of mixing reactor configuration on the concentrations of stray particles and residual particles

From the results presented in the previous section, it was found that the concentrations of stray particles and residual carbon particles varied depending on the coagulant dose. However, even if a sufficient amount of coagulant is used, if the mixing is inappropriate, a large number of stray particles may be generated due to a lack of opportunities for the particles and coagulant to come into contact. Indeed, Nakazawa et al. (2018b) have reported that the concentration of residual particles after filtration varied with the intensity and time of mixing during coagulation treatment, though the concentration of stray particles are not measured. Another important mixing condition is the distribution of residence time. The experiments of Nakazawa et al. (2018b) were conducted as batch tests, which results in a constant and uniform residence time. However, actual water treatment systems use a continuous flow reactor, which results in a residence time that varies. In other words, even if the average residence time is long enough, if the residence time has a wide variance over time, the fact that some particles may not have sufficient opportunity to come into contact with the coagulant can result in the formation of stray particles (Bratby 2006, Crittenden et al. 2012).

Thus, in the present study, we used flow-through reactors with different set-ups to investigate the effect of mixing reactor configuration on stray particle concentration. In these experiments, a single-chambered reactor or a 3-chambered reactor, with the same total HRT and same size impellors (one per chamber), was used for coagulation treatment with rapid mixing. In addition, a single-chambered reactor or a 4-chambered reactor, with the same total HRT and

same total number of impellors with the same size and rotational speed, was used for flocculation with slow mixing. According to the residence time distributions determined for the coagulation and flocculation reactors (Figs. S6 and S7), the proportion of the distributions indicating a short residence time (less than half of the HRT) was larger for the single-chambered reactor than for the 3- or 4-chambered reactors.

First, we examined the effect of coagulation reactor (rapid mixing unit) configuration on residual carbon particle concentration in sand filtrate. Although the single-chambered reactor and the 3-chambered reactor had the same mixing intensity (G value) and HRT, a lower residual carbon particle concentration was obtained with the 3-chambered reactor than with the single-chamber reactor (Fig. 5a and Fig. S8). This suggests that the different residence time distributions of the two types of reactor influenced the residual carbon particle concentration in the sand filtrate. The same trend was observed for stray particle concentrations in water sampled at the end of flocculation: use of the single-chambered coagulation reactor resulted in a higher stray particle concentration (Fig. 5b). Thus, when a large proportion of the residence time distribution included short residence times, which was observed in the distribution for the single-chambered reactor (Fig. S6 and Fig. S7), the stray particle concentration was increased, which subsequently increased the residual carbon particle concentration in the sand filtrate.

Next, we examined the effect of flocculation reactor (slow mixing unit) configuration on residual carbon particle concentration in sand filtrate (Fig. 6a and Fig. S9). The 4-chambered reactor resulted in a lower residual particle concentration in the sand filtrate than the single-chambered reactor when PACl-50 was used as the coagulant. The same trend was observed for stray particle concentration in water sampled at the end of flocculation treatment (Fig. 6b). However, when PAC-70 was used, this trend was not observed, because flocculation with slow mixing did not reduce the stray particle concentration, as discussed in the next section.

When the residual carbon particle concentration in sand filtrate was plotted against the stray particle concentration in water sampled after flocculation treatment (slow mixing), a strong positive correlation was observed (R^2 = 0.96, Fig. 7a). This supports our finding that stray particle concentration can be used as an index of residual particle concentration in sand filtrate, and that such particles are the origin of the residual carbon particles. We also examined the correlation between the residual carbon particle concentration in sand filtrate and the stray particle concentration in water collected after coagulation treatment (rapid mixing), but a correlation was lower (R^2 = 0.70; Fig. 7b). We concluded that this was because the stray particle concentration was changed slightly during the flocculation process after PACl-50 coagulation, as discussed in the next section. Similarly, we examined the correlation between the residual carbon particle concentration in sand filtrate and the turbidity of settled water sampled after sedimentation. The turbidity of settled water was not correlated with residual carbon particle concentration in sand filtrate (R^2 = 0.15; Fig. 7c), although the turbidity of settled water was found to also be influenced by the residence time distribution of

the coagulation and flocculation reactors (Fig. S10). We concluded that turbidity was not an index of the residual carbon particle concentration in the sand filtrate.

3.4. Effect of PACl type on stray particle concentration after coagulation and flocculation

The stray particle concentration was markedly decreased during coagulation treatment but left unchanged or slightly decreased by flocculation treatment (Fig. 8). More specifically, stray particle concentration was decreased by flocculation treatment with a 4-chambered-reactor slow-mixing when PACl-50, but not clearly PACl-70, was used as the coagulant. To further examine why the behavior of the stray particles during the flocculation treatment differed depending on the coagulant used, we conducted a series of batch experiments. As shown in Fig. 9, the stray carbon particles behaved differently during coagulation and flocculation depending on which coagulant was used. When PACl-70 was used, the stray particle concentration was high during the initial 20 s of rapid mixing for coagulation and was markedly decreased at 100 s of rapid mixing. During the subsequent slow mixing for flocculation, the concentration remained unchanged. This trend was also held for raw water with high NOM (natural organic matter) concentration (DOC: 3.8 mg/L), though stray particle concentrations were generally high due to the consumption of coagulant by NOM (DOC after SPAC dose was 3.7 mg/L and DOC after SPAC and coagulant doses was 2.5 mg/L) (Bratby 2006). In contrast, when PACl-50 was used, the stray particle concentration was lower at 20 s of rapid mixing compared with that when PACl-70 was used, and it then gradually decreased until the end of slow mixing.

We also examined the relationship between the behavior of the stray carbon particles and the distributions of the aluminum species derived from the coagulants. Fig. 10 shows the changes in the Al species distributions for PACl-70 and PACl-50 during rapid mixing ($G = 381\ s^{-1}$) and slow mixing ($G = 8\ s^{-1}$). The stock solution of PACl-50 contained 42% Ala, 23% Alb, and 35% Alc. When PACl-50 was added to water and hydrolyzed, almost no Ala remained at 20 s from the beginning of rapid mixing, and the amount of Alb increased to become the dominant species. Alb remained the dominant species until the second half of the slow mixing. In contrast, the stock solution of PACl-70 contained 25% Ala, 14% Alb, and Alc, 61%. When PACl-70 was added to water and hydrolyzed, as for PACl-50, almost no Ala remained at 20 s from the beginning of rapid mixing. However, unlike for PACl-50, Alc remained the dominant species throughout the rapid and slow mixing processes.

Considering that PACl-70 markedly decreased the concentration of stray particles within several tens of seconds from the beginning of rapid mixing, unlike PACl-50, the present data suggest that the reactive hydrolysis product formed from Alc contributed to the rapid decrease of stray particles after only a short period of mixing. However, the stray particle concentration was not decreased further after rapid mixing, probably because the reactive hydrolysis product was fast-acting but unstable, which could easily transform into unreactive products, although the unreactive product was still categorized as Alc. When using PACl-70, rapid dispersion of the short-lived reactive hydrolysis product formed from Alc may be key for reducing the

number of stray particles. This interpretation is consistent with our previously reported finding that PACl-70 needs rapid, intense mixing to reduce the concentration of residual particles after CSF (Nakazawa et al. 2018b).

In contrast to PACl-70, PACl-50 decreased stray particles less during rapid mixing because of lower Alc content. PACl-50 contained more Ala and Alb, the latter of which is reported to be effective for charge neutralization but have poor floc-forming ability (Yan *et al.* 2008). During slow mixing, the concentration of Alb decreased measurably by 15%, and the concentration of Alc increased in response. Therefore, this newly formed reactive Alc might contribute to the decrease of stray particles observed during slow mixing when PACl-50 was used. Therefore, it is expected that the stray particle concentration will be reduced even during slow mixing for flocculation if multiple stages of slow mixing are used. However, the formation of reactive Alc from Alb in slow mixing is slow, and then the decrease of stray particles is only slight.

3.5. Fate and removal of stray particles by sand filtration

As shown in Figs. 3 and 7, the concentrations of stray particles in water sampled after coagulation and flocculation were much higher than the residual particle concentrations in the sand filtrate. Furthermore, we found that stray particles are able to pass through the flocculation and sedimentation processes with only a slight decrease in their concentration (Fig. S11). Assuming that the source of the residual particles in the sand filtrate was stray particles (see the discussion in Section 3.2), most, but not all, of them are removed by sand filtration.

When we calculated the removal rate of particles by particle size using the stray particle concentration in water sampled after sedimentation and the residual carbon particle concentrations in sand filtrate, we found that the removal rate of stray particles was in the range of 60%–90% for particles with a diameter of 0.3 to 2.0 μm (Fig. 11). There are many models that can be used to estimate the removal rate of fine particles by sand filtration. We used three representative models [RT model (Rajagopalan and Tien 1976), TE model (Tufenkji and Elimelech 2004), and Yao model (Yao *et al.* 1971)] presented by Crittenden et al. (2012) to estimate the removal rate of particles with a size of 0.3 to 2 μm, which included both the stray particles and the residual particles in sand filtrate. The modeled removal rates, 15%–55% for the particles with sizes of 0.3–2 μm (Fig. S12), were much lower than the experimentally observed values of 60%–90%. Since the theoretical models assume a filtration media of spherical particles of uniform size, which is quite different from actual filters, it is not surprising that the experimental and calculated removal rates did not agree. Nevertheless, these findings suggest that a removal rate >60% would be achieved for particles with a diameter of 0.3 to 2 μm. This suggests that some of the particles categorized as stray particles were easily removed by sand filtration. We imagine that such particles might be actually larger in size than the size of the particles observed under the microscope because the aluminum, which attaches to the particles and neutralizes their charge, is transparent and does

not appear in microphotographs. As already discussed in Section 3.2, zeta potential measurement revealed that the stray particles had less negative-charge than did the residual carbon particles in sand filtrate, which indicates that most of the stray particles were more charge-neutralized by the attachment of a larger amount of aluminum. This suggests that the true size of stray particles is likely to be larger than the apparent grain size observed under the microscope. Therefore, the removal efficiency of such particles would be higher than expected according to apparent particle size and filtration theory. In addition, we imagine that among the stray particles there are particles with much-less charge-neutralization and that these much-less-charge-neutralized, stray particles are able to easily pass through the sand filter and reach the filtrate. Thus, in future studies it will be important to evaluate not only particle size diversity but also charge diversity rather than rely only on average values. Such examinations will allow us to more efficiently control the carbon particle residual after CSF treatment.

4. Conclusions

Our conclusions from the present research are as follows:

1) In a CSF process using SPAC, the residual carbon concentration in the sand filtrate was dramatically decreased with time during the initial 2 h of filtration due to filter ripening, and a filtrate quality of <200 particles/mL was achieved. The size distribution of the residual carbon particles in the sand filtrate was not changed during the filter-ripening period, suggesting an increase in the efficiency of particle attachment rather than transport to the sand surface during this period. Therefore, charge-destabilization rather than particle size is likely key for minimizing residual particles.

2) Stray carbon particles, which were determined as the particles remaining in the centrifugal supernatant of the water sampled after rapid mixing for coagulation and slow mixing for flocculation, were less charge-neutralized than the bulk particles. The concentration of stray particles dropped markedly during rapid mixing process, and then it was unchanged or only slightly decreased during slow mixing and sedimentation processes. The concentrations of stray carbon particles in water sampled after rapid/slow mixing processes for coagulation/flocculation were well correlated with the residual carbon particle concentrations in sand filtrate, but the turbidity of water entering the sand filter water was not.

3) Among the bulk particles, stray particles, which account for less than 0.4% of the bulk particles, could be a major source of residual particles in sand filtrate due to their lower charge neutralization. Therefore, a goal of the coagulation treatment process should be to reduce the stray particle concentration.

4) Optimizing reactor configurations and the type and dose of coagulant were effective for reducing stray particle and residual carbon particle concentrations in sand filtrate. PACl-70 performed better with a multi-chambered reactor than with a single-chambered reactor for coagulation with rapid mixing. In contrast, PACl-50 performed better with a multi-chambered reactor than with a single-chambered reactor for both coagulation with rapid mixing and

flocculation with slow mixing. The performance requirements of the reactors for coagulation and flocculation were related to the predominant aluminum species in the coagulant: Alc of PACl-70 is fast-acting, whereas Ala of PACl-50 is slow-acting.

Acknowledgments

This work was supported by a Grant-in-Aid for Scientific Research S [grant number JP16H06362] and a JSPS Research Fellowship [grant number JP19J11070] from the Japan Society for the Promotion of Science.

References

Aguilar, M.I., Sáez, J., Lloréns, M., Soler, A. and Ortuño, J.F. (2003) Microscopic observation of particle reduction in slaughterhouse wastewater by coagulation–flocculation using ferric sulphate as coagulant and different coagulant aids. Water Research 37(9), 2233-2241.

Amaral, P., Partlan, E., Li, M., Lapolli, F., Mefford, O.T., Karanfil, T. and Ladner, D.A. (2016) Superfine powdered activated carbon (S-PAC) coatings on microfiltration membranes: Effects of milling time on contaminant removal and flux. Water Research 100, 429-438.

Apul, O.G., Hoogesteijn von Reitzenstein, N., Schoepf, J., Ladner, D., Hristovski, K.D. and Westerhoff, P. (2017) Superfine powdered activated carbon incorporated into electrospun polystyrene fibers preserve adsorption capacity. Science of The Total Environment 592, 458-464.

Ateia, M., Erdem, C.U., Ersan, M.S., Ceccato, M. and Karanfil, T. (2019) Selective removal of bromide and iodide from natural waters using a novel AgCl-SPAC composite at environmentally relevant conditions. Water Research 156, 168-178.

Bonvin, F., Jost, L., Randin, L., Bonvin, E. and Kohn, T. (2016) Super-fine powdered activated carbon (SPAC) for efficient removal of micropollutants from wastewater treatment plant effluent. Water Research 90, 90-99.

Bratby, J. (2006) Coagulation and Flocculation in Water and Wastewater Treatment, IWA Publishing.

Crittenden, J.C., Trussell, R.R., Hand, D.W., Howe, K.J. and Tchobanoglous, G. (2012) MWH's Water Treatment Principles and Design, Third Edition, John Wiley & Sons, Inc.

Decrey, L., Bonvin, F., Bonvin, C., Bonvin, E. and Kohn, T. (2020) Removal of trace organic contaminants from wastewater by superfine powdered activated carbon (SPAC) is neither affected by SPAC dispersal nor coagulation. Water Research 185, 116302.

Ding, Q., Yamamura, H., Murata, N., Aoki, N., Yonekawa, H., Hafuka, A. and Watanabe, Y. (2016) Characteristics of meso-particles formed in coagulation process causing irreversible membrane fouling in the coagulation-microfiltration water treatment. Water Research 101, 127-136.

555 Edzwald, J.K. (2011) WATER QUALITY & TREATMENT A Handbook on Drinking
556 Water, American Water Works Association, American Society of Civil Engineers, McGraw-
557 Hill.
558 Hu, C.-Y., Lo, S.-L., Chang, C.-L., Chen, F.-L., Wu, Y.-D. and Ma, J.-l. (2013) Treatment of
559 highly turbid water using chitosan and aluminum salts. Separation and Purification
560 Technology 104, 322-326.
561 Huang, X., Wan, Y., Shi, B. and Shi, J. (2020) Effects of powdered activated carbon on the
562 coagulation-flocculation process in humic acid and humic acid-kaolin water treatment.
563 Chemosphere 238, 124637.
564 Kanaya, S., Kawase, Y., Mima, S., Sugiura, K., Murase, K. and Yonekawa, H. (2015)
565 Drinking Water Treatment Using Superfine PAC (SPAC): Design and Successful Operation
566 History in Full-scale Plant, pp. 624-631, Salt Lake City, Utah, USA.
567 Kimura, M., Matsui, Y., Kondo, K., Ishikawa, T.B., Matsushita, T. and Shirasaki, N. (2013)
568 Minimizing residual aluminum concentration in treated water by tailoring properties of
569 polyaluminum coagulants. Water Research 47(6), 2075-2084.
570 Kobayashi, S., Matsui, Y., Nakazawa, Y., Shinno, K., Abe, T., Matsushita, T. and Shirasaki,
571 N. (2019) Survey of Residual Concentration of Powdered Activated Carbon in Rapid Sand
572 Filtration System - Using Automatic Carbon Particles Counting Method (in Japanese), Japan
573 Water Works Association, Hakodate, Hokkaido, Japan.
574 Lee, B.-B., Choo, K.-H., Chang, D. and Choi, S.-J. (2009) Optimizing the coagulant dose to
575 control membrane fouling in combined coagulation/ultrafiltration systems for textile
576 wastewater reclamation. Chemical Engineering Journal 155(1), 101-107.
577 Matsui, Y., Aizawa, T., Kanda, F., Nigorikawa, N., Mima, S. and Kawase, Y. (2007)
578 Adsorptive removal of geosmin by ceramic membrane filtration with super-powdered
579 activated carbon. Journal of Water Supply: Research and Technology—AQUA 56(6-7), 411-
580 418.
581 Matsui, Y., Hasegawa, H., Ohno, K., Matsushita, T., Mima, S., Kawase, Y. and Aizawa, T.
582 (2009) Effects of super-powdered activated carbon pretreatment on coagulation and trans-
583 membrane pressure buildup during microfiltration. Water Research 43(20), 5160-5170.
584 Matsui, Y., Nakao, S., Taniguchi, T. and Matsushita, T. (2013) Geosmin and 2-
585 methylisoborneol removal using superfine powdered activated carbon: shell adsorption and
586 branched-pore kinetic model analysis and optimal particle size. Water Research 47(8), 2873-
587 2880.
588 Murray, C.C., Vatankhah, H., McDonough, C.A., Nickerson, A., Hedtke, T.T., Cath, T.Y.,
589 Higgins, C.P. and Bellona, C.L. (2019) Removal of per- and polyfluoroalkyl substances using
590 super-fine powder activated carbon and ceramic membrane filtration. Journal of Hazardous
591 Materials 366, 160-168.
592 Nakazawa, Y., Matsui, Y., Hanamura, Y., Shinno, K., Shirasaki, N. and Matsushita, T.
593 (2018a) Identifying, counting, and characterizing superfine activated-carbon particles
594 remaining after coagulation, sedimentation, and sand filtration. Water Research 138, 160-168.
595 Nakazawa, Y., Matsui, Y., Hanamura, Y., Shinno, K., Shirasaki, N. and Matsushita, T.
596 (2018b) Minimizing residual black particles in sand filtrate when applying super-fine

powdered activated carbon: Coagulants and coagulation conditions. Water Research 147, 311-320.
Pan, L., Takagi, Y., Matsui, Y., Matsushita, T. and Shirasaki, N. (2017) Micro-milling of spent granular activated carbon for its possible reuse as an adsorbent: Remaining capacity and characteristics. Water Research 114, 50-58.
Partlan, E., Ren, Y., Apul, O.G., Ladner, D.A. and Karanfil, T. (2020) Adsorption kinetics of synthetic organic contaminants onto superfine powdered activated carbon. Chemosphere 253, 126628.
Rajagopalan, R. and Tien, C. (1976) Trajectory analysis of deep-bed filtration with the sphere-in-cell porous media model. AIChE Journal 22(3), 523-533.
Sun, S., Weber-Shirk, M. and Lion, L.W. (2016) Characterization of Flocs and Floc Size Distributions Using Image Analysis. Environmental Engineering Science 33(1), 25-34.
Tufenkji, N. and Elimelech, M. (2004) Correlation Equation for Predicting Single-Collector Efficiency in Physicochemical Filtration in Saturated Porous Media. Environmental Science & Technology 38(2), 529-536.
Wang, D., Sun, W., Xu, Y., Tang, H. and Gregory, J. (2004) Speciation stability of inorganic polymer flocculant–PACl. Colloids and Surfaces A: Physicochemical and Engineering Aspects 243(1), 1-10.
Yan, M., Wang, D., Ni, J., Qu, J., Chow, C.W. and Liu, H. (2008) Mechanism of natural organic matter removal by polyaluminum chloride: effect of coagulant particle size and hydrolysis kinetics. Water Research 42(13), 3361-3370.
Yao, K.-M., Habibian, M.T. and O'Melia, C.R. (1971) Water and waste water filtration. Concepts and applications. Environmental Science & Technology 5(11), 1105-1112.
Younker, J.M. and Walsh, M.E. (2016) Effect of adsorbent addition on floc formation and clarification. Water Research 98, 1-8.
Yu, W.-z., Qu, J.-h. and Gregory, J. (2015) Pre-coagulation on the submerged membrane fouling in nano-scale: Effect of sedimentation process. Chemical Engineering Journal 262, 676-682.
Zhang, P., Wu, Z., Zhang, G., Zeng, G., Zhang, H., Li, J., Song, X. and Dong, J. (2008) Coagulation characteristics of polyaluminum chlorides PAC-Al30 on humic acid removal from water. Separation and Purification Technology 63(3), 642-647.

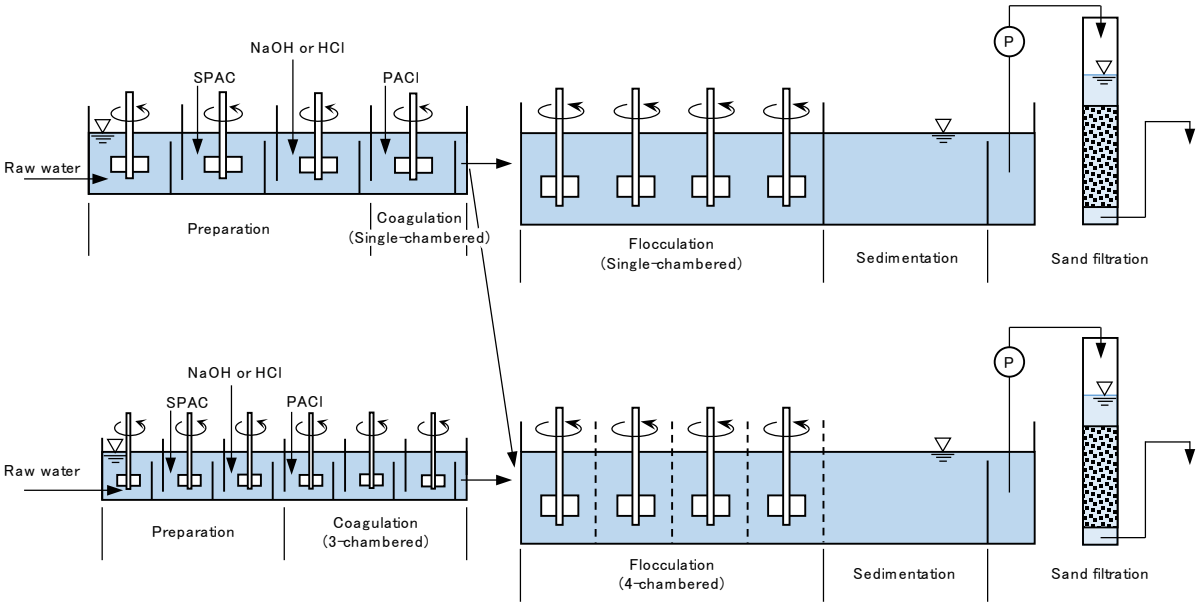

Fig. 1. Schematic diagram of the bench-scale CSF plant.

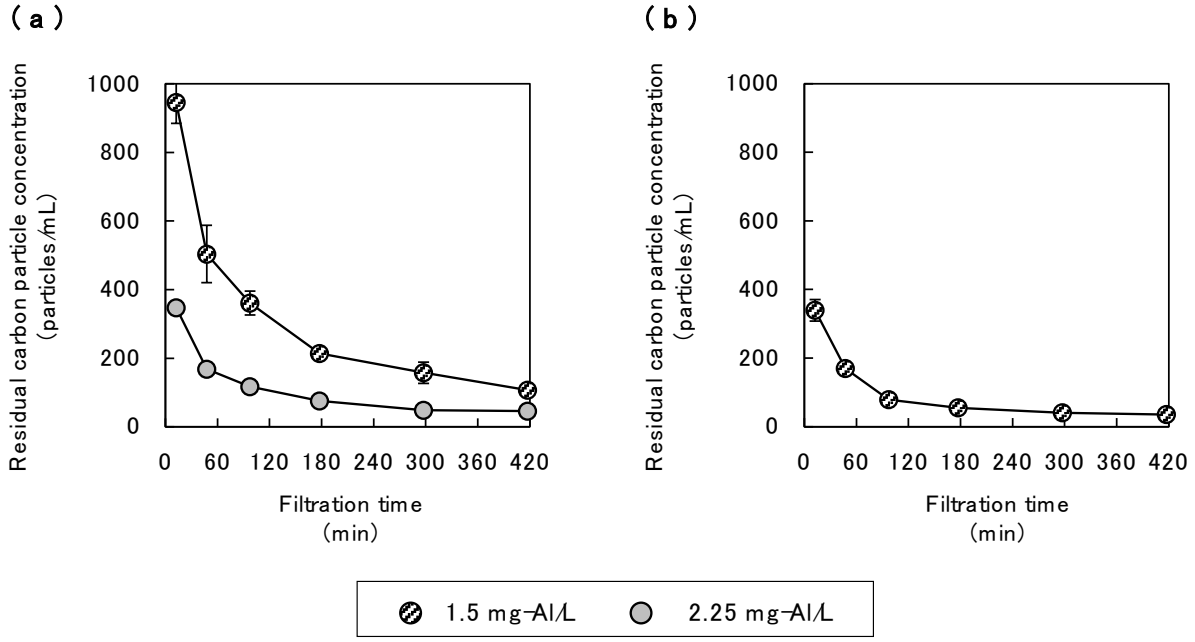

Fig. 2. Residual carbon particle concentration in sand filtrate after treatment of river water (a, River water 1) or municipal water (b, Municipal water 1) with a bench-scale CSF plant. Coagulation: single-chambered reactor, G = 600 s^{-1}; flocculation: 4-chambered reactor, G = 12.5 s^{-1}; filtration rate, 90 m d^{-1}. SPAC initial concentration, 2.0 mg/L; coagulant (PACl-70), 1.5 or 2.25 mg-Al/L. Error bars indicate standard deviations of 3 measurements, but some of them are hidden behind the symbols.

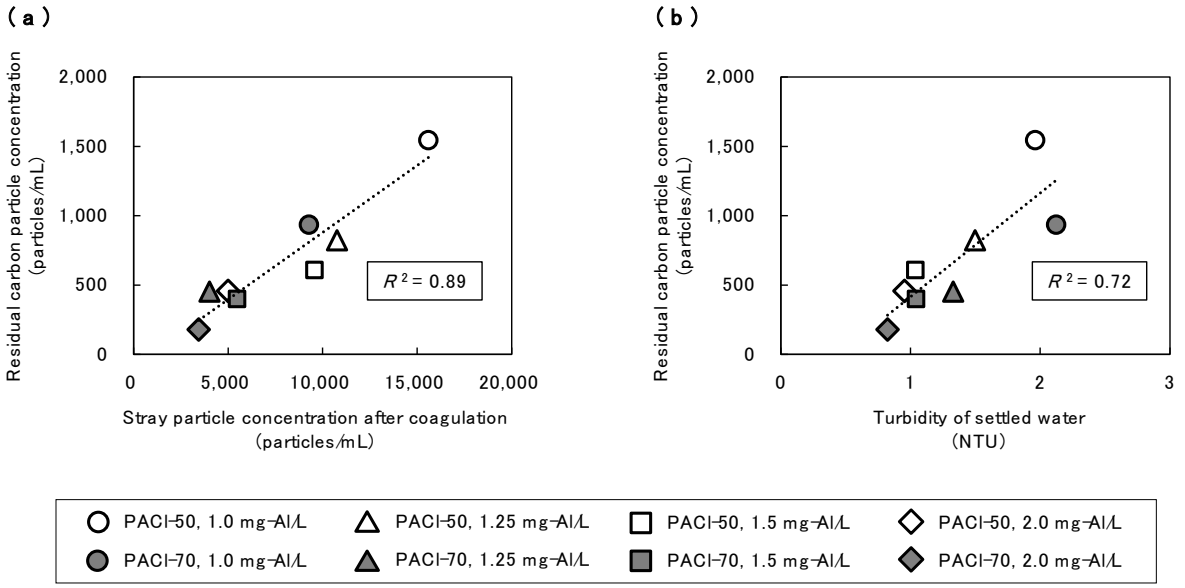

Fig. 3. Correlation between residual carbon particle concentration in sand filtrate and stray carbon particle concentration after coagulation with rapid mixing (a), and between residual carbon particle concentration of sand filtrate and turbidity of settled water (b). Municipal water 2 (PACl-70) or Municipal water 3 (PACl-50) was used as the raw water. SPAC initial concentration, 2.0 mg/L. Coagulant (PACl-50 or PACl-70), 1.0, 1.25, 1.5, or 2.0 mg-Al/L. Coagulation, single-chambered reactor, G = 600 s^{-1}; flocculation, 4-chambered reactor, G = 12.5 s^{-1}; filtration rate, 90 m d^{-1}.

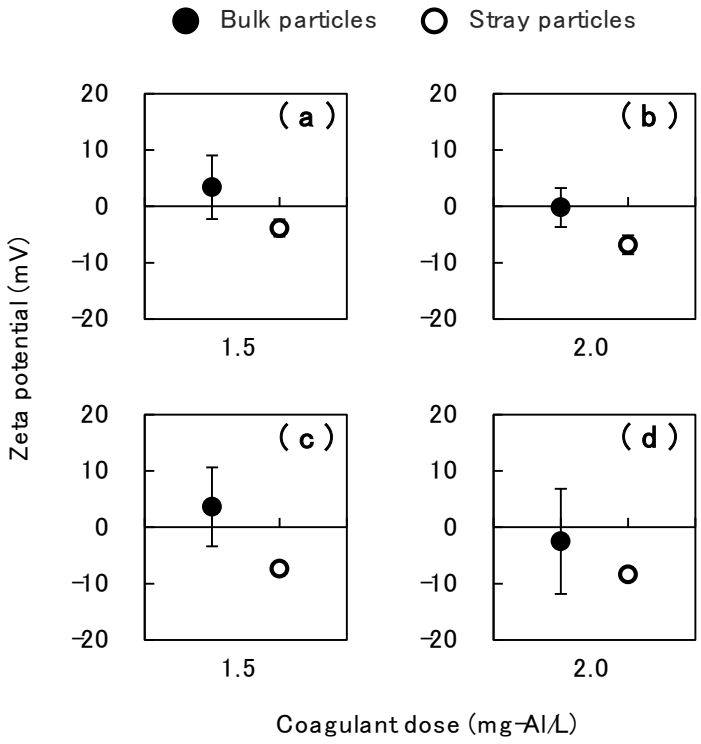

Fig. 4. Comparison of the zeta potentials of bulk particles and stray carbon particles after coagulation. Water samples were collected after coagulation with rapid mixing. The zeta potentials of bulk particles were determined for each sample without further processing. The zeta potentials of the stray particles were determined after the samples were subjected to centrifugal separation. Municipal water 4 was used as the raw water. SPAC initial concentration, 2.0 mg/L; coagulant, PACl-70 (a, b) or PACl-50 (c, d), 1.5 or 2.0 mg-Al/L. This was a batch-type coagulation test using a 1-L rectangular beaker and a mixing velocity of G = 600 s^{-1}. The error bars represent standard deviations of 7−11 measurements, but some of them are hidden behind the symbols.

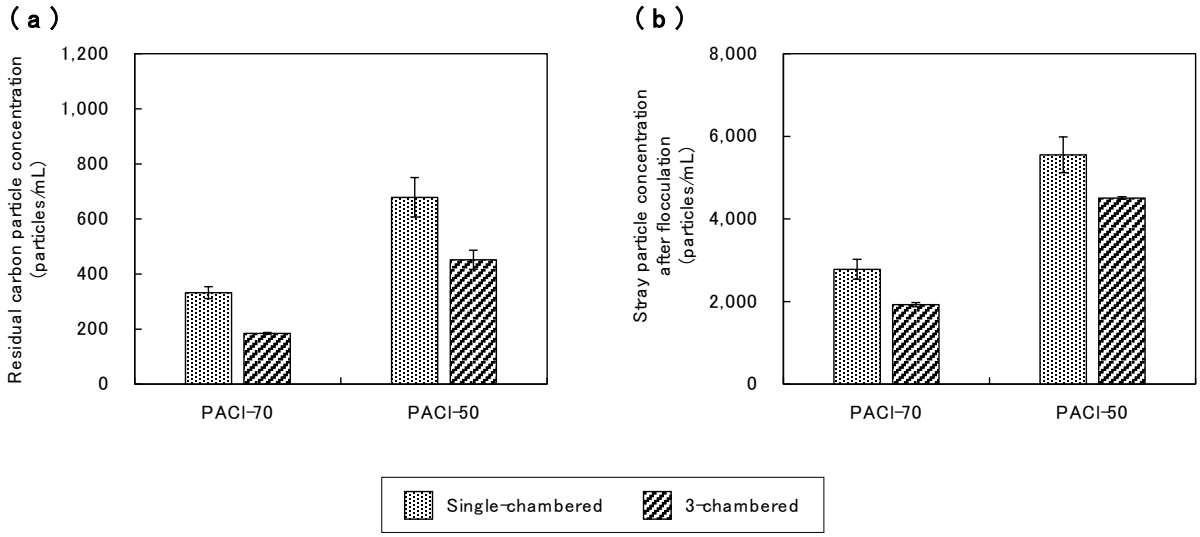

Fig. 5. Effect of rapid mixing reactor configuration (a single-chambered or 3-chambered coagulation reactor) on (a) residual particle concentration in sand filtrate and (b) stray particle concentration in water sampled after flocculation. Both reactors used the same mixing intensity (G = 600 s^{-1}) and same total HRT (100 s), and were followed by a 4-chambered flocculation reactor (G = 12.5 s^{-1}) and a sand filter. Municipal water 5 was used as the raw water. SPAC initial concentration, 2.0 mg/L; coagulant (PACl-50 or PACl-70), 1.5 mg-Al/L; filtration rate, 90 m d^{-1}. Error bars indicate standard deviations of 3 measurements.

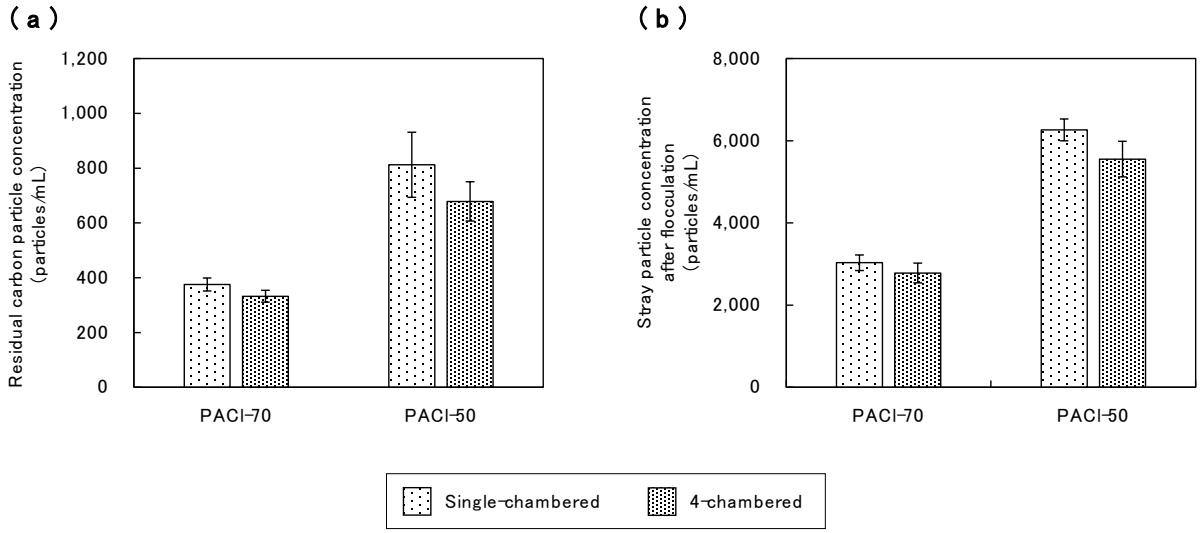

Fig. 6. Effect of slow mixing reactor configuration (a single-chambered or 4-chambered flocculation reactor) on (a) residual particle concentration in sand filtrate and (b) stray carbon particle concentration in water sampled after flocculation. Both reactors used the same mixing intensity ($G = 12.5\ s^{-1}$) and same total HRT (2400 s) and were preceded by a single-chambered coagulation reactor ($G = 600\ s^{-1}$). The experimental conditions were the same as described in the caption to Fig. 5. Error bars indicate standard deviations of 3 measurements.

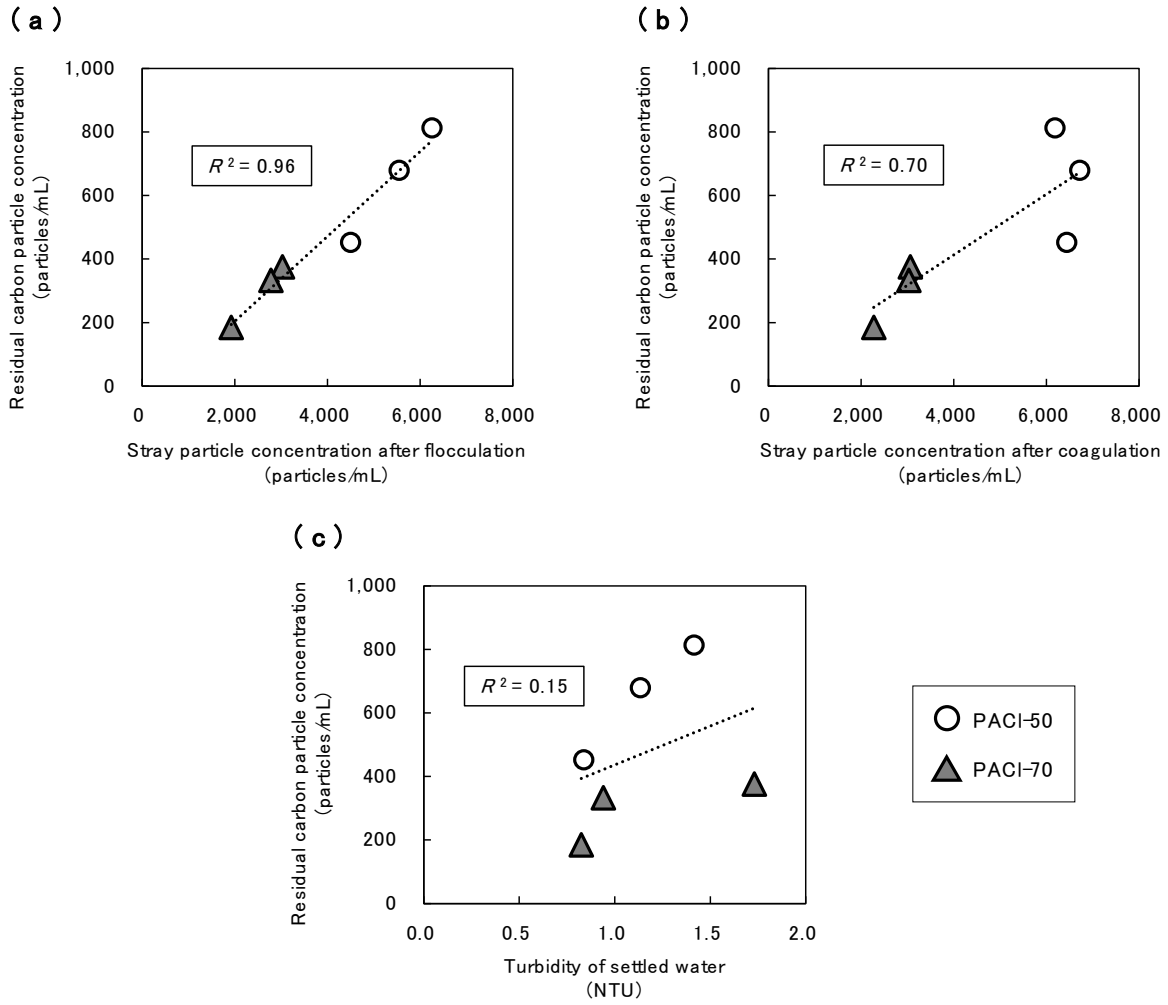

Fig. 7. Correlations between residual carbon particle concentration in sand filtrate and stray particle concentration in water sampled after flocculation with slow mixing (a), stray particle concentration in water after coagulation with rapid mixing (b), and turbidity of settled water (c). The experimental conditions were the same as described in the captions to Figs. 5, 6, and S10, respectively.

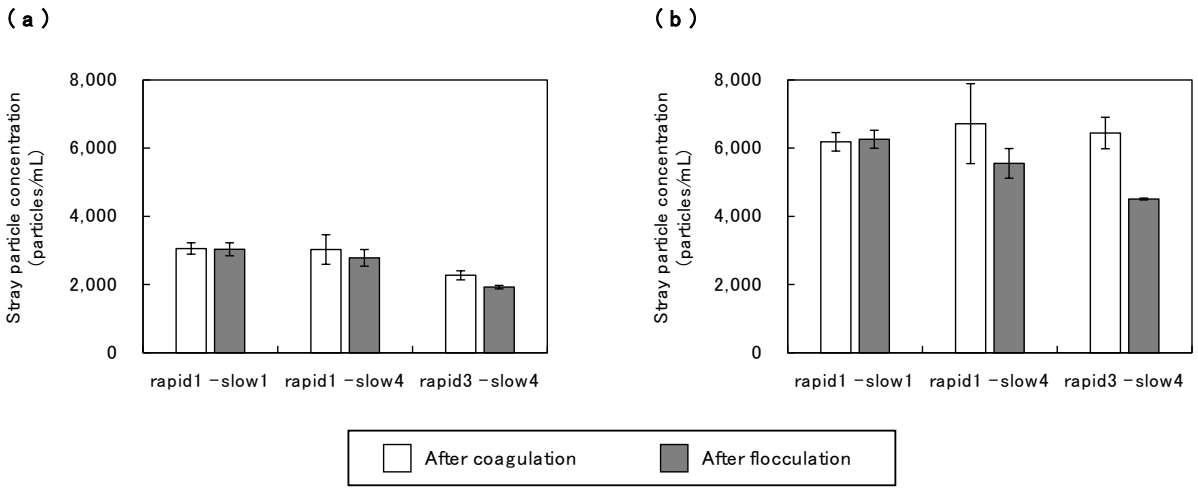

Fig. 8. Change in stray particle concentration after coagulation and flocculation. On the horizontal axis, the numbers after "rapid" and "slow" indicate the number of chambers in the coagulation and flocculation reactors, respectively. Coagulation was conducted with rapid mixing (G = 600 s^{-1}, 100 s). Flocculation was conducted with slow mixing (G = 12.5 s^{-1}, 2400 s). SPAC initial concentration, 2 mg/L. PACl-70 (a) or PACl-50 (b) was used as the coagulant. The experimental conditions were the same as described in the caption to Figs. 5 and 6.

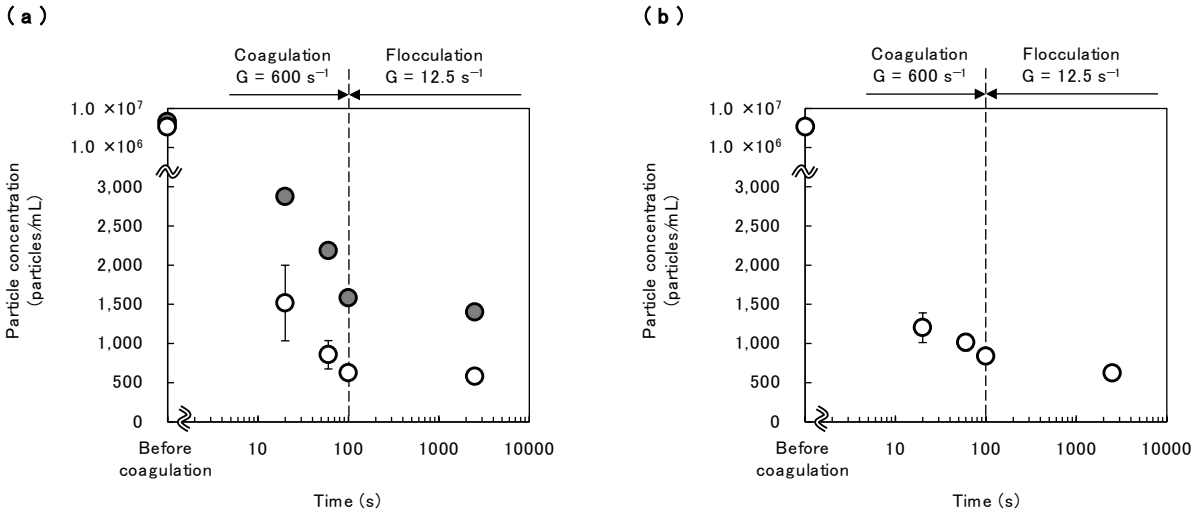

Fig. 9. Change of particle concentration against mixing time during coagulation and flocculation. Batch experiments were conducted using a 1-L rectangular beaker, Municipal water 1 (white plots) or River water 2 (grey plots) as the raw water, and PACl-70 (a) or PACl-50 (b) at 1.5 mg-Al/L as the coagulant. SPAC initial concentration, 2.0 mg/L. Water samples were collected during coagulation and flocculation treatments and then subjected to centrifugal separation treatment (see Section 2.4). Centrifugal supernatants were examined for carbon particle concentration. Water sampled before coagulation was also examined. Two runs were conducted for Municipal water 1, and one run for River water 2. Error bars represent the standard deviations for experiments, but some of them are hidden behind the symbols.

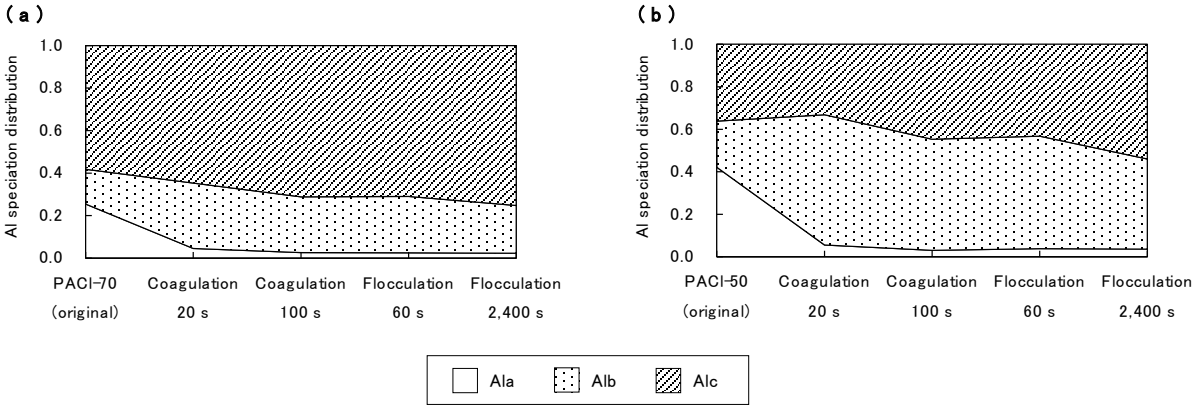

Fig. 10. Change in Al species distribution of PACl by coagulation and flocculation. PACl-70 (a) and PACl-50 (b) were hydrolyzed at 270 mg-Al/L in Municipal water 1 without carbon particles. Batch-type coagulation tests were conducted using a 1-L rectangular beaker. "original" means the Al speciation distribution of the PACl stock solution. "Coagulation" refers to coagulation with rapid mixing ($G = 381\ s^{-1}$); "Flocculation" refers to flocculation with slow mixing ($G = 8\ s^{-1}$). Ala, Alb, and Alc are monomeric, polymeric, and colloidal species, respectively.

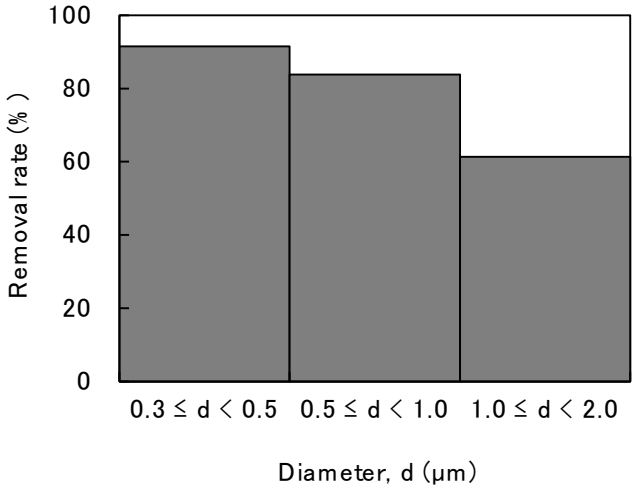

Fig. 11. Removal rate of carbon particles in three size classes by sand filtration. Removal rate was calculated between the stray particle concentration in water sampled after sedimentation and the residual carbon particle concentration in sand filtrate. River water 1 was used as the raw water. Coagulant (PACl-70) dose, 2.25 mg-Al/L. The experimental conditions were the same as described in the caption to Fig. 2.

Supplementary Information

Stray particles as the source of residuals in sand filtrate: Behavior of superfine powdered activated carbon particles in water treatment processes

Yoshifumi Nakazawa [a], Taketo Abe [a], Yoshihiko Matsui [b]*, Nobutaka Shirasaki [b], and Taku Matsushita [b]

[a] Graduate School of Engineering, Hokkaido University, N13W8, Sapporo 060-8628, Japan
[b] Faculty of Engineering, Hokkaido University, N13W8, Sapporo 060-8628, Japan

* Corresponding author. Tel./fax: +81-11-706-7280
E-mail address: matsui@eng.hokudai.ac.jp

Ferron method for aluminum speciation in poly-aluminum chloride

In the Ferron method, Ala denotes aluminum species that react with Ferron within 30 s, which are mainly monomeric Al species. Alb denotes Al species that react with Ferron from 30 s to 120 min, which are mainly polymeric Al species. Alc denotes Al species that do not react with Ferron, which are mainly colloidal Al species. The Ferron analyses of the poly-aluminum chlorides (PACls) were conducted immediately after diluting each PACl with pure water (Milli-Q water; Milli-Q Advantage A10 System; Merck KGaA, Darmstadt, Germany) to 0.27 g-Al/L (0.01 mol-Al/L). Absorbance at 366 nm was measured using a glass cell that had a 10-cm optical path length. Dilution is reported to have little effect on the Ferron assay for PACl (Kimura *et al.* 2013).

Wet ball and wet bead milling to produce superfine powdered activated carbon

First, a powdered activated carbon (PAC) slurry (31% w/w) was prepared by admixing a commercially available wood-based PAC (Taiko W; Futamura Chemical Co., Ltd., Nagoya, Japan) with Milli-Q water. This slurry was transferred to a closed-chamber ball mill (Nikkato, Osaka, Japan) including 5- and 10-mm-diameter Al_2O_3 balls as the disintegrating media, and the PAC was pulverized at 45–50 rpm for 6 h to reduce its D95 (the diameter where 95% of the entire distribution lies below) to less than 30 μm. After that, the slurry was moved to a bead mill system (LMZ015; Ashizawa Finetech, Ltd., Chiba, Japan). The bead mill system was operated in circulation mode with 0.3-mm-diameter ZrO_2 beads, and the carbon particles in the suspension were further pulverized at a rotational speed of 8 m s^{-1} (2590 rpm) for 30 min to produce a superfine powdered activated carbon (SPAC) slurry.

The particle size distribution of the SPAC was determined as follows. A portion of SPAC slurry was added to a dispersant (Triton X-100; Kanto Chemical Co., Inc., Tokyo, Japan; final concentration, 0.08% w/v) and sonicated at 150 W for 1 min to thoroughly disperse the carbon particles. Then, the size distribution was measured by using a laser light diffraction and scattering method (Microtrac MT3300EXII; MicrotracBEL Corp., Osaka, Japan).

Membrane filtration and microscopic image analysis to determine carbon particle concentration and particle size

The concentrations and particle sizes of carbon particles were determined by membrane filtration and microscopic image analysis. Carbon particles in water samples were captured on a membrane filter (nominal pore diameter, 0.1 μm; Φ25 mm; polytetrafluoroethylene; Merck KGaA). After the filter was left to dry naturally at room temperature, color digital photomicrographs of the filter surface were recorded under a digital microscope (VHX-2000; Keyence Corporation, Osaka, Japan) at 1000× magnification. The number of observation zones (9, 10, or 18 per

filter; microscope view area, 247 μm × 330 μm) were predetermined depending on particle concentration (Nakazawa *et al.* 2018). Finally, the photomicrographs were analyzed by using the image analysis software associated with the microscope and the particle concentration, and the sizes calculated were represented by the surface-equivalent sphere diameter. The analytical procedures are reported in detail elsewhere (Nakazawa et al. 2018).

Flow-through coagulation–flocculation, sedimentation, and sand filtration experiment

The plant comprised five components: preparation unit, coagulation reactor (rapid mixing), flocculation reactor (slow mixing), sedimentation reactor, and sand filter (Fig. 1 and Table S1). Coagulation was conducted using a single-chambered reactor or a 3-chambered-reactor with three equally-sized chambers; the two reactors had the same total hydraulic retention time (HRT) of 100 s. Flocculation was conducted using a single-chambered reactor or a 4-chambered reactor, both with four mixing impellers and the same total HRT of 2400 s. Regardless of reactor configuration, coagulation was conducted with rapid mixing at a fixed mixing intensity (G value: velocity gradient) of 600 s^{-1} for 100 s, and flocculation was conducted with slow mixing at a fixed G value of 12.5 s^{-1} for 2400 s. Residence time distributions of the reactors were measured by tracer test using NaCl as the tracer and conductivity detection (Crittenden et al. 2012). All chemicals and raw water were fed into the plant via peristaltic pumps at constant flow rates.

Toyohira River water, collected at Moiwa Water Purification Plant, Sapporo, Japan (hereafter 'River water 1') was used as the raw water. We also used dechlorinated Sapporo municipal water (Municipal waters 1–3 and 5–7) because only a limited volume of River water was available (Table S2). The raw waters were stored in a tank (130 or 500 L) and then pumped into the first mixing chamber of the preparation unit at 0.5 L/min. SPAC was added to the second mixing chamber of the preparation unit at a concentration of 2 mg/L, which is a typical dose when SPAC is used as an adsorbent (Nakayama *et al.* 2020).

After the addition of NaOH (0.05 N) or HCl (0.05 N) to adjust the final coagulation pH to 7.0 in the third chamber of the preparation unit, coagulant (PACl) was injected into the coagulation reactor; when the 3-chambered reactor was used for coagulation, the coagulant was injected into the first chamber. The coagulant dose was 1.5 mg-Al/L, unless otherwise noted, and it was predetermined to bring the settling turbidity to less than 1.0 NTU. Samples of water were collected from the outlet of the coagulation reactor and from the outlet of the flocculation reactor for the determination of non-coagulated carbon particle concentration, as described in Sections 2.1 and 2.4, respectively.

After flocculation, the water flowed through a sedimentation unit, which had a HRT of 60 min, and a portion of the supernatant was sampled for the determination of turbidity (2100Q portable turbidimeter; Hach Company, Loveland, CO, USA). In some cases, a portion of supernatant was sampled for the determination of stray carbon particle concentration.

After sedimentation, the supernatant was transferred to a sand filter. Sand filtration was conducted at a rate of 90 or 150 m d^{-1} in the down-flow direction using a 4-cm diameter column filled with sand (effective diameter, 0.94 mm; uniformity, 1.24; Nihon Genryo Co., Ltd., Japan) to a depth of 50 cm. After the start of filtration, sand filtrates were collected from 0 to 25, from 35 to 60, from 85 to 110, from 165 to 190, from 285 to 310, and from 405 to 430 min, representing filtration times of 12.5, 47.5, 97.5, 178, 298, and 418 min, respectively, and used to determine turbidity and carbon particle concentration. After each filtration run, the sand filter was backwashed with municipal water and then washed forward with Milli-Q water before the next filtration run.

Table. S1. Specifications of the bench-scale coagulation–flocculation, sedimentation, and rapid sand filtration plant.

Component	Type	Number of chambers	Length × width × height per chamber	Water depth	Volume per chamber	Hydraulic retention time per chamber	G value
			cm	cm	L	s	s^{-1}
Preparation unit	Connected to the single-chambered coagulation reactor	3	9.5 × 9.5 × 15	9.2	0.83	100	600
	Connected to the 3-chambered coagulation reactor	3	6.6 × 6.6 × 12	6.4	0.28	33	600
Coagulation reactor	Single-chambered reactor	1	9.5 × 9.5 × 15	9.2	0.83	100	600
	3-chambered reactor	3	6.6 × 6.6 × 12	6.4	0.28	33	600
Flocculation reactor	Single-chambered reactor	1	56 × 19 × 25	19	20	2400	12.5
	4-chambered reactor	4	14 × 19 × 25	19	5	600	12.5

Component	Length × width × height	Water depth	Volume	Hydraulic retention time	Overflow rate
	cm	cm	L	s	mm min^{-1}
Sedimentation reactor	88 × 19 × 25	19	32	3900	3.0

Component	Outer diameter of column	Inner diameter of column	The column to particle diameter ratio	Length of column	Effective diameter of sand	Uniformity coefficient of sand	Sand depth	Filtration rate
	cm	cm		cm	mm		cm	m d^{-1}
Sand filter	4.0	3.6	40	140 or 90	0.94	1.24	50	90 or 150

Table. S2. Raw waters used in the present study.

Raw water	Turbidity	Black particle concentration	DOC	Alkalinity	Na^+	K^+	Mg^{2+}	Ca^{2+}	Cl^-	NO_3^-	SO_4^{2-}	
	NTU	particles/mL	mg/L	mg/L as CaCO3	mg/L	mg/L	mg/L	mg/L	mg/L	mg/L	mg/L	
River water 1	2.3	no data	0.8	16	12	2.1	1.8	10	21	1.5	20	Fig. 2 (a), Fig. 11, Fig. S1 (a, b), Fig. S11
River water 2	13	16	3.8	76	44	6	9	19	19	<0.14	6	Fig. 9
Municipal water 1	0.1	15	0.6	18	15	2.3	2.4	11	23	0.8	21	Fig. 2 (b), Fig. 9, Fig. 10, Fig. S1 (c)
Municipal water 2	0.1	no data	0.5	20	17	2.6	2.1	10	24	1	19	Fig. 3 (PACl-70), Fig. S3 (PACl-70), Fig. S4 (PACl-70), Fig. S5 (PACl-70)
Municipal water 3	0.1	no data	0.6	20	18	2.6	1.6	11	28	0.8	19	Fig. 3 (PACl-50), Fig. S3 (PACl-50), Fig. S4 (PACl-50), Fig. S5 (PACl-50)
Municipal water 4	no data	no data	0.4	20	12	0.8	2.4	7	11	0.9	18	Fig. 4
Municipal water 5	0.1	no data	no data	16	13	1.7	1.8	9	23	0.9	18	Fig. 5, Fig. 6, Fig. 7, Fig. 8, Fig. S2, Fig. S10
Municipal water 6	0.1	no data	0.4	20	11	0.8	3.1	8	14	1.3	19	Fig. S8
Municipal water 7	0.1	no data	0.5	20	12	1.6	2.4	11	18	1	19	Fig. S9

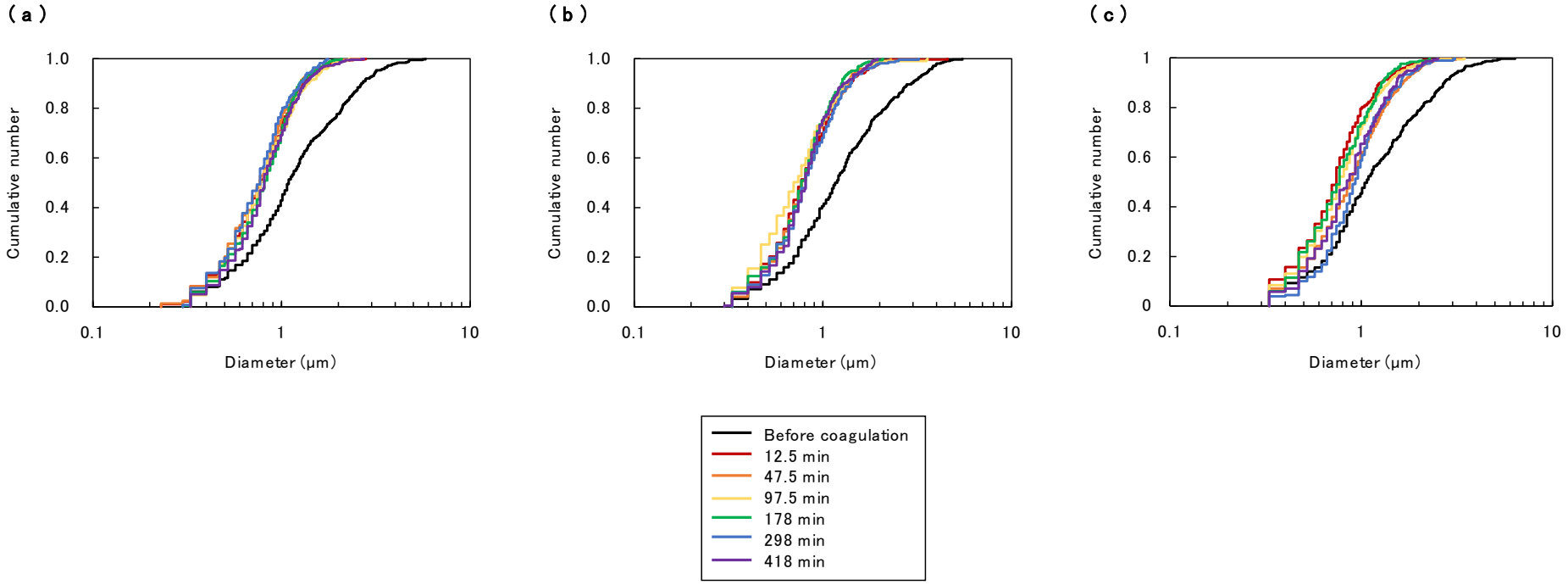

Fig. S1. Particle size distributions of carbon particles in water sampled from the preparation unit before coagulation or in sand filtrate. The numbers in the legend indicate the filtration time. Particle sizes were determined by using membrane filtration and microscopic image analysis. River water 1 (a, b) or Municipal water 1 (c) was used as the raw water. Coagulant (PACl-70) dose, 1.5 mg-Al/L (a, c) or 2.25 mg-Al/L (b). The experimental conditions were the same as those described in the caption to Fig. 2.

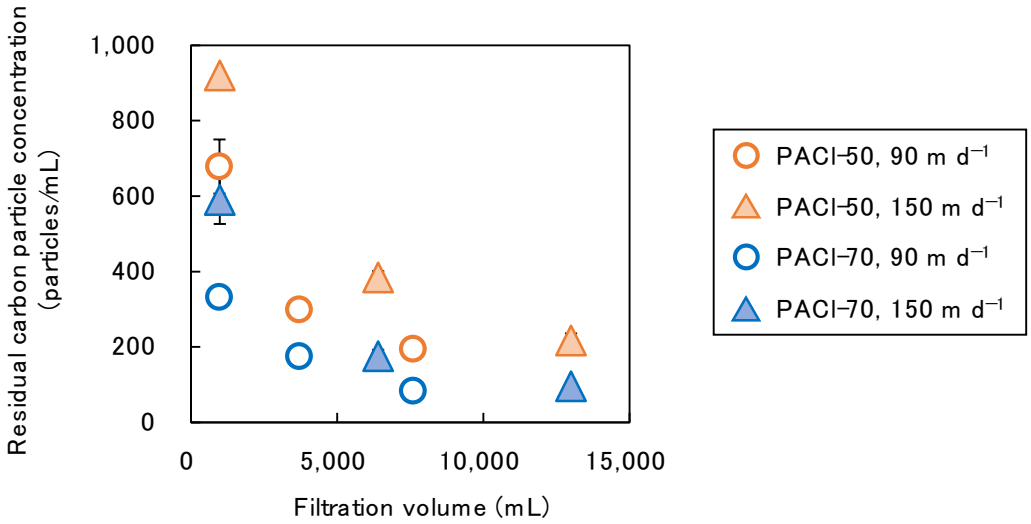

Fig. S2. Effect of filtration rate on residual particle concentration in sand filtrate. Filtration rate, 90 or 150 m d^{-1}. Municipal water 5 was used as the raw water. SPAC initial concentration, 2.0 mg/L; coagulant (PACl-50 or PACl-70), 1.5 mg-Al/L. Coagulation, single-chambered reactor, G = 600 s^{-1}; flocculation, 4-chambered reactor, G = 12.5 s^{-1}.

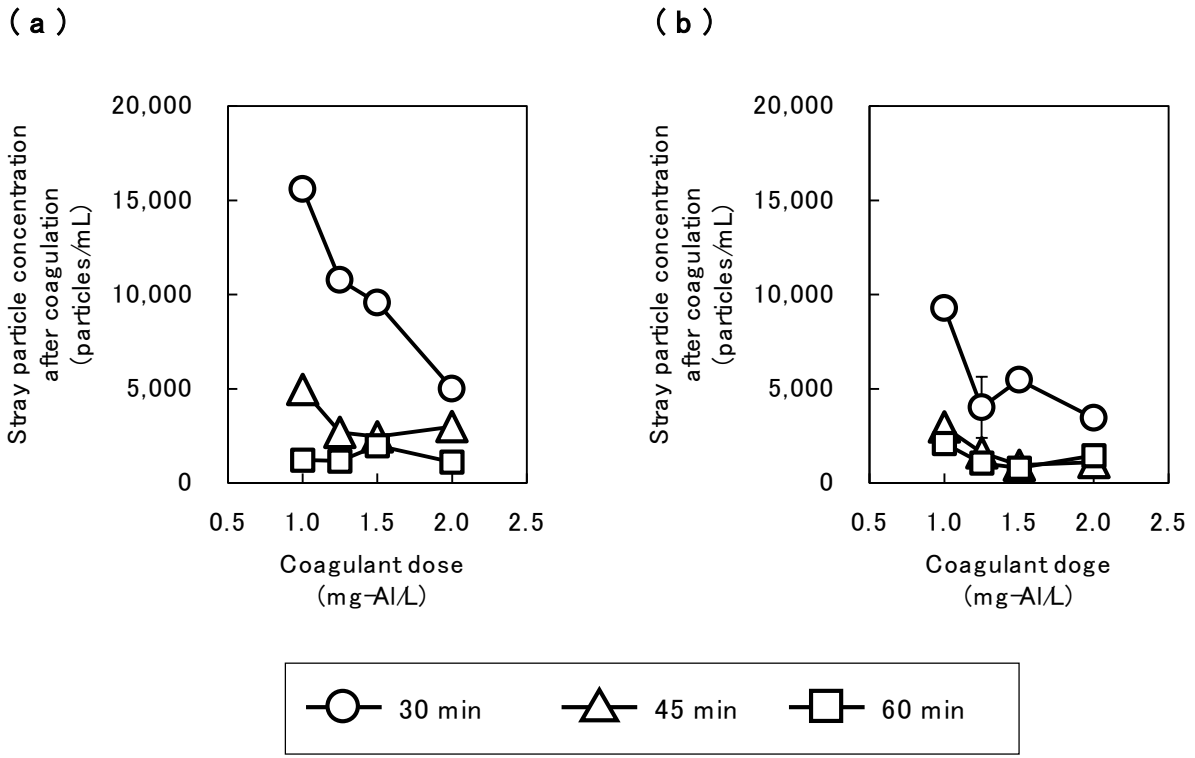

Fig. S3. Effect of coagulant dose on stray carbon particle concentration after coagulation with rapid mixing. PACl-50 (a) or PACl-70 (b) was used as the coagulant. Stray particles were collected from water sampled after coagulation by using a double-centrifugation method to remove floc particles. Total centrifugation times were 30 min (circles), 45 min (triangles), and 60 min (squares). Municipal water 2 (PACl-70) or Municipal water 3 (PACl-50) was used as the raw water. SPAC initial concentration, 2.0 mg/L. Coagulation, single-chambered reactor, G = 600 s^{-1}.

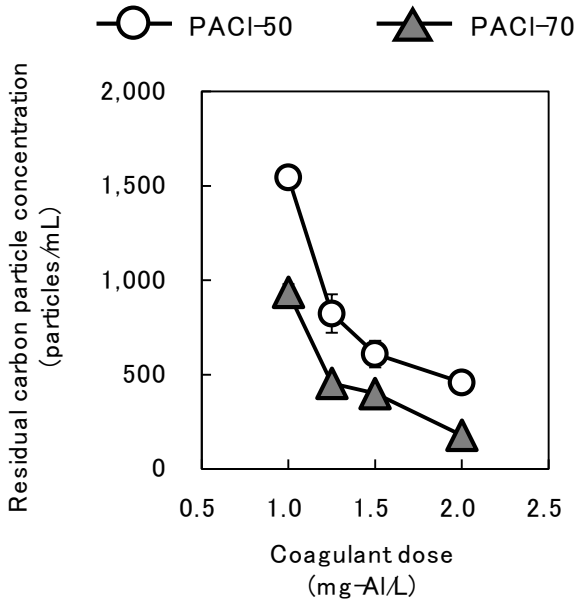

Fig. S4. Effect of coagulant dose on residual carbon particle concentration in sand filtrate. PACl-50 or PACl-70 was used as the coagulant at 1.0, 1.25, 1.5, or 2.0 mg-Al/L. Municipal water 2 (PACl-70) or Municipal water 3 (PACl-50) was used as the raw water. SPAC initial concentration, 2.0 mg/L. Coagulation, single-chambered reactor, G = 600 s^{-1}; flocculation, 4-chambered reactor, G = 12.5 s^{-1}; filtration rate, 90 m d^{-1}. The experimental conditions were the same as described in the caption to Fig. 3.

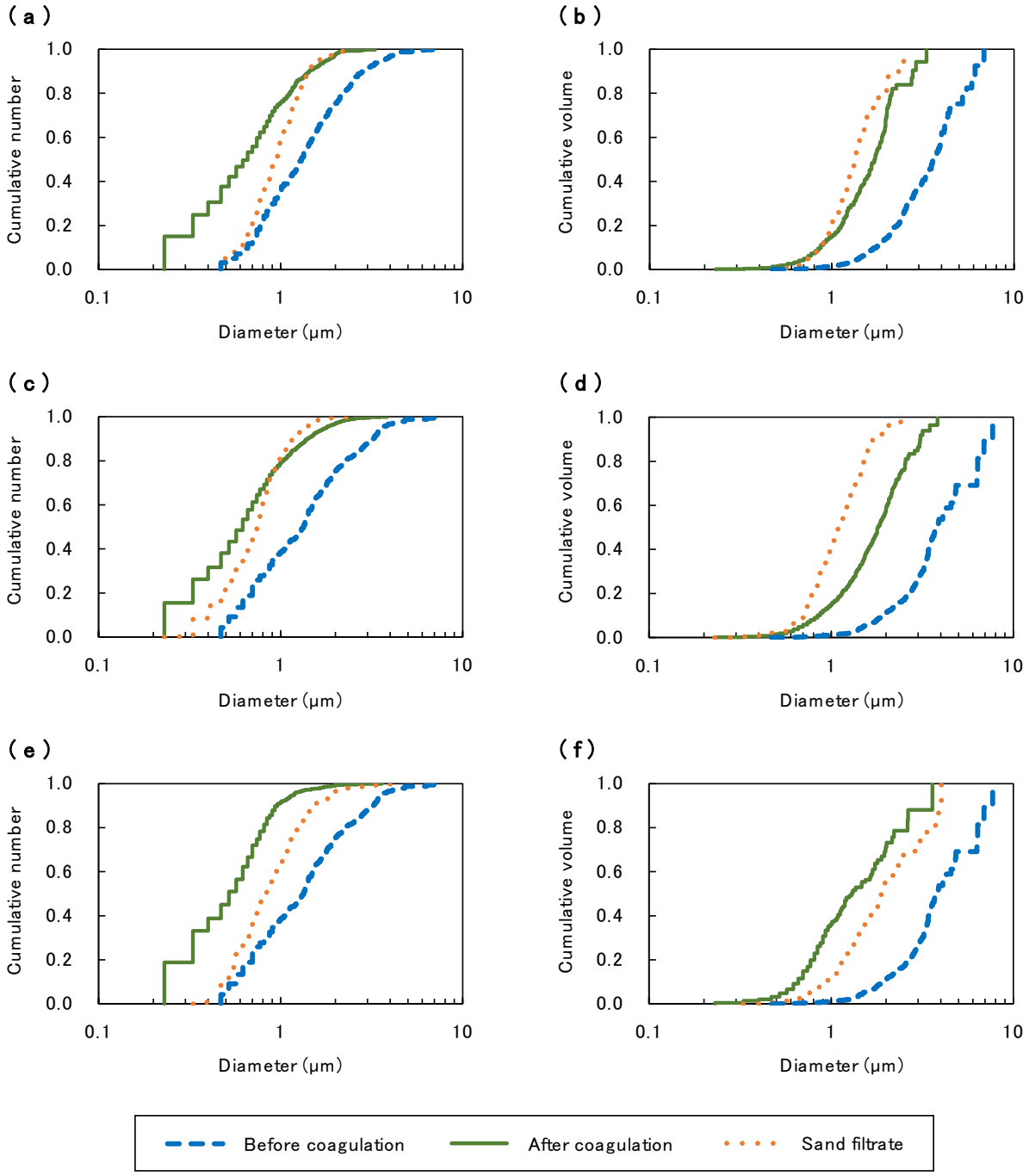

Fig. S5. Particle size distributions of carbon particles in water samples; cumlative number (a, c, e) or cumlative volume (b, d, f). Water samples were collected after coagulation, subjected to centrifugal separation treatment (see Section 2.4), and the supernatants were examined for particle size distribution. Water sampled before coagulation and sand filtrate were also examined. Particle sizes were determined by using membrane filtration and microscopic image analysis. Municipal water 2 (a, b) or Municipal water 3 (c, d, e, f) was used as the raw water. SPAC initial concentration, 2.0 mg/L. Coagulant, PACl-70 (a, b) or PACl-50 (c, d, e, f), 1.5 mg-Al/L (c, d) or 2.0 mg-Al/L (a, b, e, f). The experimental conditions were the same as described in the caption to Fig. 3.

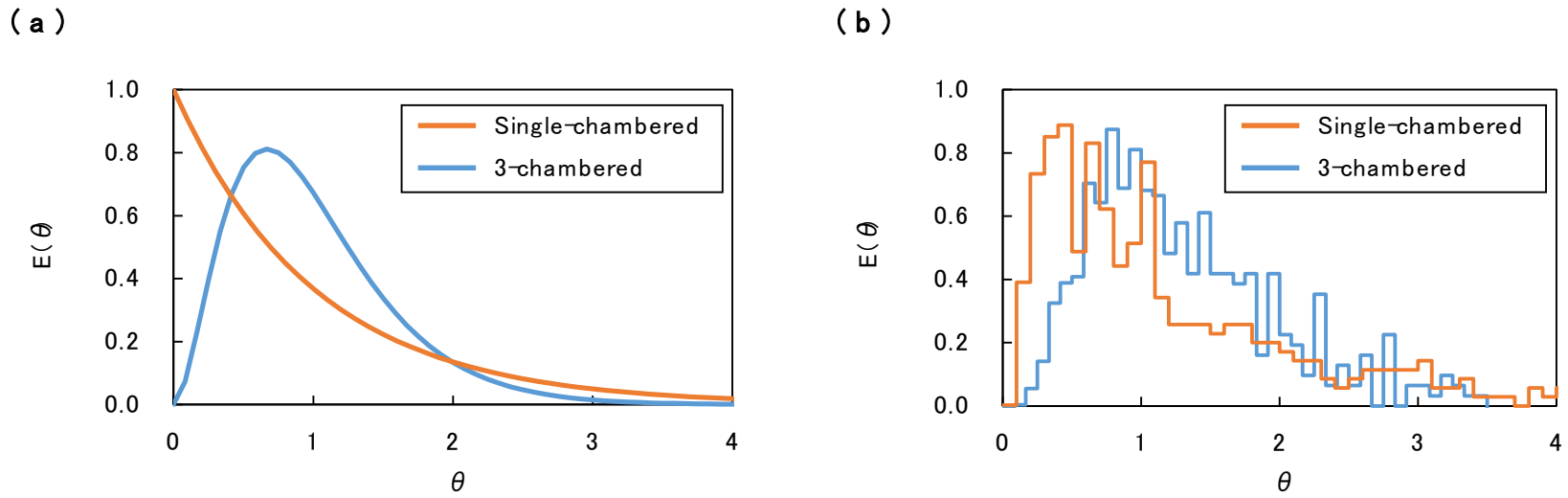

Fig. S6. Theoretical (a) and experimental (b) residence time distributions for the single-chambered or 3-chambered coagulation reactor with rapid mixing. θ is normalized residence time divided by HRT, and E(θ) is residence time distribution (Crittenden et al. 2012).

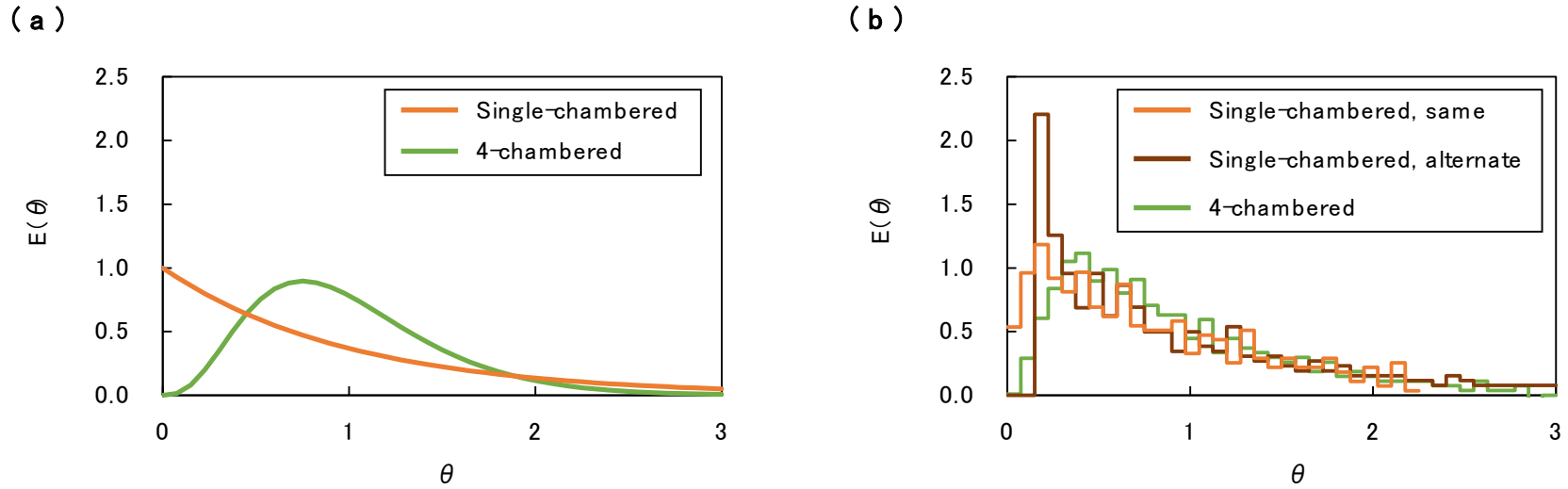

Fig. S7. Theoretical (a) and experimental (b) residence time distributions for the single-chambered or 4-chambered flocculation reactor with slow mixing. “alternate” means that the direction of rotation of the 4 mixers alternated; “same” means that the direction of rotation of the 4 mixers was the same. θ is normalized residence time, time divided by HRT, and E(θ) is residence time distribution (Crittenden et al. 2012).

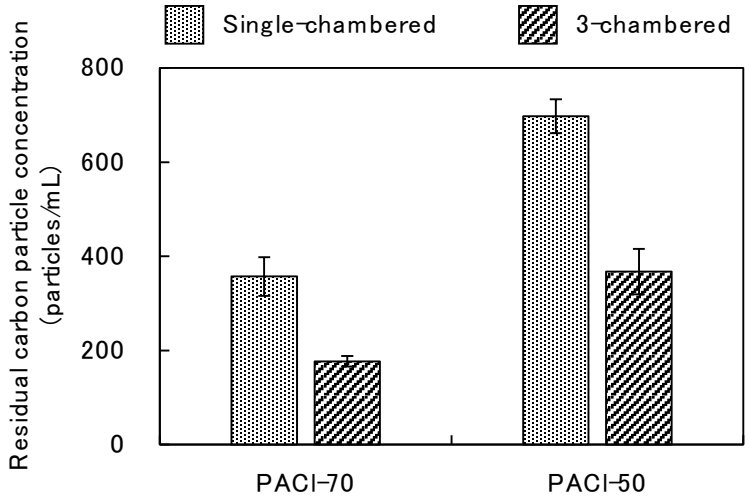

Fig. S8. Effect of coagulation reactor configuration on residual carbon particle concentration in sand filtrate. A single-chambered or 3-chambered coagulation reactor with the same mixing intensity (G = 600 s^{-1}) and same total HRT (100 s) was used. Both reactors were followed by a 4-chambered flocculation reactor (G = 12.5 s^{-1}) and a sand filter. Municipal water 6 was used as the raw water. SPAC initial concentration, 2.0 mg/L; coagulant (PACl-50 or PACl-70), 1.5 mg-Al/L; filtration rate, 90 m d^{-1}.

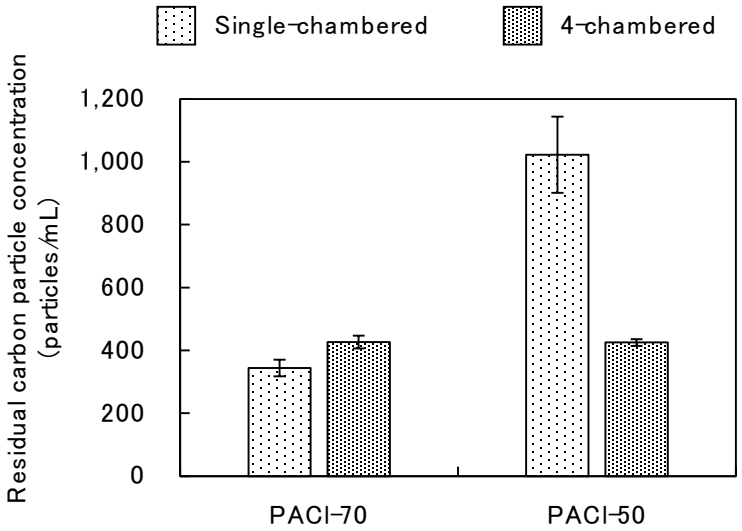

Fig. S9. Effect of flocculation reactor configuration on residual particle concentration in sand filtrate. A single-chambered coagulation reactor (G value of 600 s^{-1}) followed by a single-chambered or 4-chambered flocculation reactor with the same mixing intensity (G = 12.5 s^{-1}) and same total HRT (2400 s) were used. Municipal water 7 was used as the raw water. SPAC initial concentration, 2.0 mg/L; coagulant (PACl-50 or PACl-70), 1.5 mg-Al/L; filtration rate, 90 m d^{-1}.

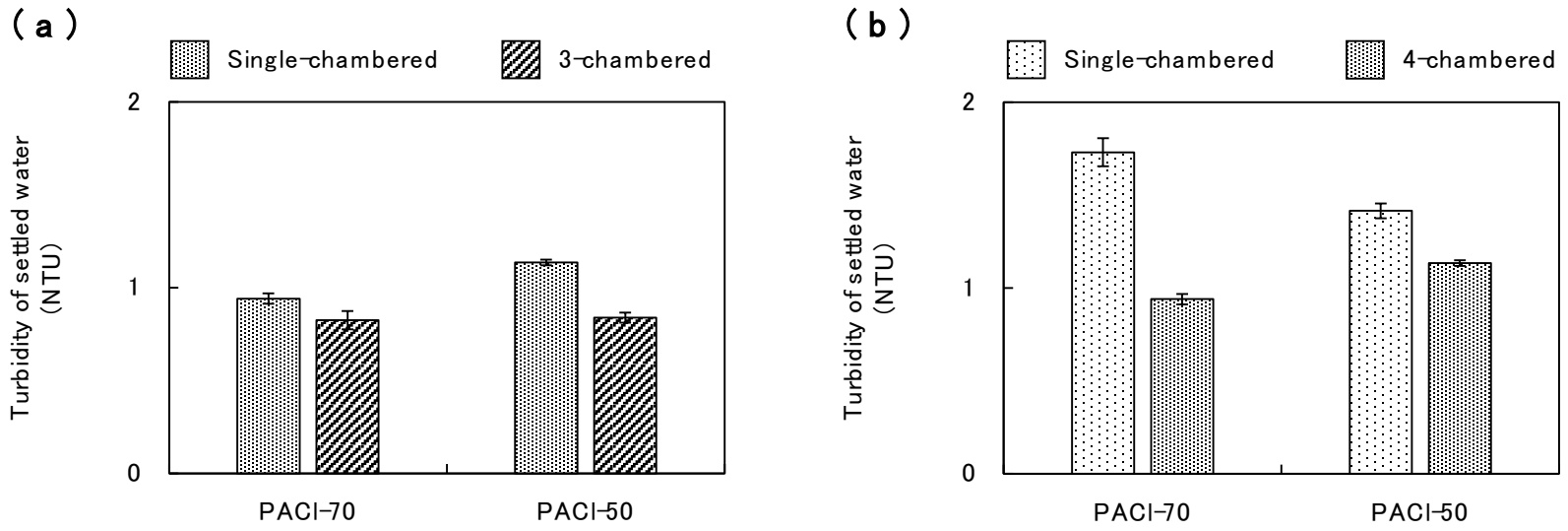

Fig. S10. Effect of mixing reactor configuration on the turbidity of settled water after sedimentation. (a) Effect of a single-chambered or 3-chambered coagulation reactor. Both reactors used the same mixing intensity (G = 600 s^{-1}) and the same total HRT (100 s) and were followed by a 4-chambered flocculation reactor (G = 12.5 s^{-1}). (b) Effect of a single-chambered or 4-chambered flocculation reactor. Both reactors used the same mixing intensity (G = 12.5 s^{-1}) and same total HRT (2400 s) and were preceded by a single-chambered coagulation reactor (G = 600 s^{-1}). Municipal water 5 was used as the raw water. SPAC initial concentration, 2.0 mg/L; coagulant (PACl-50 or PACl-70), 1.5 mg-Al/L; settling time, 65 min. The experimental conditions were the same as described in the caption to Figs. 5 and 6.

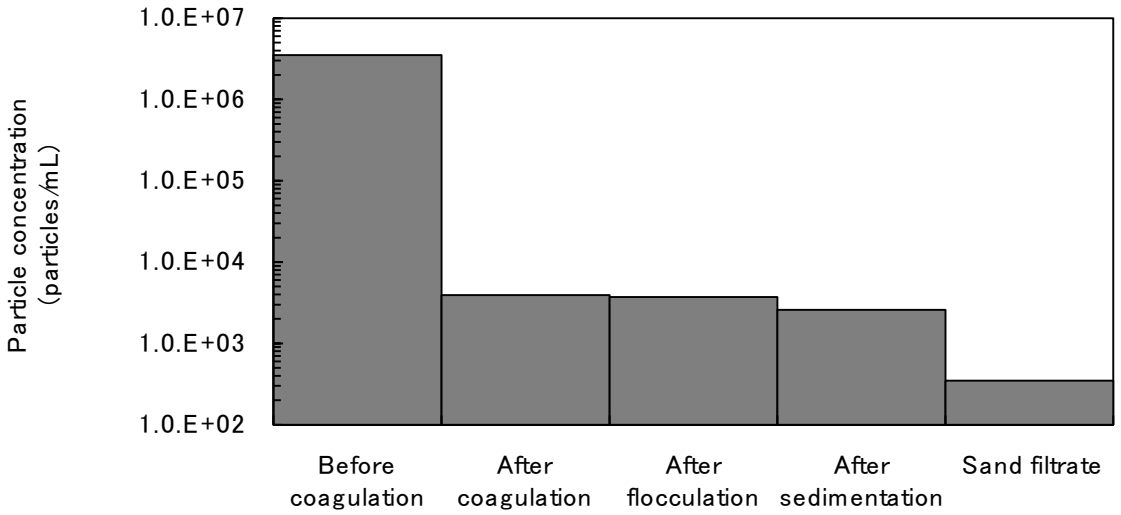

Fig. S11. Change in carbon particle concentration during the CSF process. Water samples were collected after coagulation, after flocculation, and after sedimentation, subjected to centrifugal separation treatment (see Section 2.4), and the supernatants were examined for carbon particle concentration. Water sampled before coagulation and sand filtrate were also examined. River water 1 was used as the raw water. Coagulant (PACl-70) dose, 2.25 mg-Al/L. The experimental conditions were the same as described in the caption to Fig. 2.

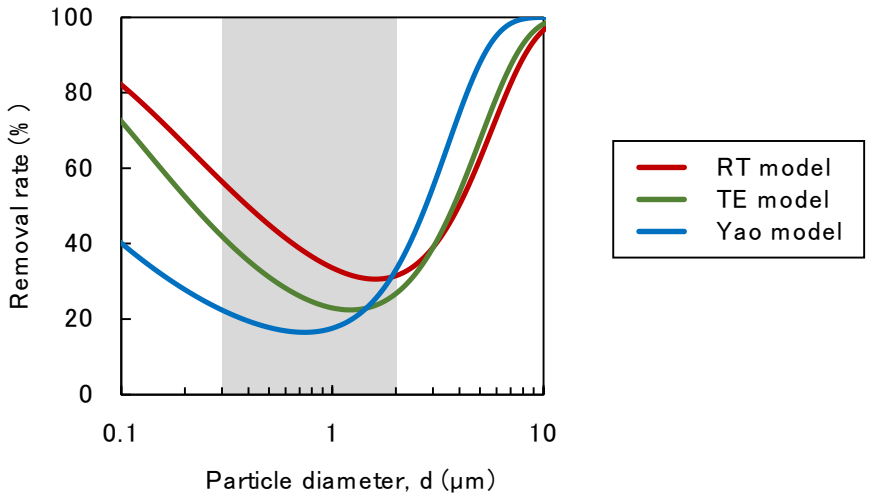

Fig. S12. Theoretical rates of particle removal by sand filtration, as determined by three different models. Removal rates were calculated by using the three models [RT model (Rajagopalan and Tien 1976), TE model (Tufenkji and Elimelech 2004), and Yao model (Yao *et al.* 1971)] and the following parameters: collector diameter (effective diameter of sand), dc = 0.94 mm; filtration rate, v = 3.75 m/h; temperature, T = 20 °C; particle density, ρ_P = 1,330 kg/m^3; depth of filter, L = 0.5 m; bed porosity, ε = 0.40; and Hamaker constant, $Ha = 1.73 \times 10^{-20}$, geometric mean of *Ha* values of activated carbon (Chen and Huang 2017) and quartz (Adamczyk 2017). In the figure, the grey band (particle diameter, 0.3–2 μm) shows the particle size range for the stray particles and residual carbon particles in sand filtrates in the present study.

References

Adamczyk, Z. (2017) Particles at Interfaces, Interactions, Deposition, Structure, Academic Press.

Chen, C. and Huang, W. (2017) Aggregation kinetics of nanosized activated carbons in aquatic environments. Chemical Engineering Journal 313, 882-889.

Kimura, M., Matsui, Y., Kondo, K., Ishikawa, T.B., Matsushita, T. and Shirasaki, N. (2013) Minimizing residual aluminum concentration in treated water by tailoring properties of polyaluminum coagulants. Water Research 47(6), 2075-2084.

Nakayama, A., Sakamoto, A., Matsushita, T., Matsui, Y. and Shirasaki, N. (2020) Effects of pre, post, and simultaneous loading of natural organic matter on 2-methylisoborneol adsorption on superfine powdered activated carbon: Reversibility and external pore-blocking. Water Research 182, 115992.

Nakazawa, Y., Matsui, Y., Hanamura, Y., Shinno, K., Shirasaki, N. and Matsushita, T. (2018) Identifying, counting, and characterizing superfine activated-carbon particles remaining after coagulation, sedimentation, and sand filtration. Water Research 138, 160-168.

Rajagopalan, R. and Tien, C. (1976) Trajectory analysis of deep-bed filtration with the sphere-in-cell porous media model. AIChE Journal 22(3), 523-533.

Tufenkji, N. and Elimelech, M. (2004) Correlation Equation for Predicting Single-Collector Efficiency in Physicochemical Filtration in Saturated Porous Media. Environmental Science & Technology 38(2), 529-536.

Yao, K.-M., Habibian, M.T. and O'Melia, C.R. (1971) Water and waste water filtration. Concepts and applications. Environmental Science & Technology 5(11), 1105-1112.